CHARACTERIZING ZOOPLANKTON AND MICRONEKTON DIEL VERTICAL MIGRATION AT THE WESTERN PUERTO RICAN SHELF/SLOPE BREAK

By

Wilson Rovira Peña

A thesis submitted in partial fulfillment of the requirements for the degree of

MASTER OF MARINE SCIENCES
IN
BIOLOGICAL OCEANOGRAPHY

UNIVERSITY OF PUERTO RICO
MAYAGÜEZ CAMPUS
2006

Approved by:

_____	_____
Jorge R. García-Sais, Ph.D. Chairman, Graduate Committee	Date
_____	_____
Jorge E. Capella, Ph.D. Member, Graduate Committee	Date
_____	_____
Roy A. Armstrong, Ph.D. Member, Graduate Committee	Date
_____	_____
Mónica Alfaro, Ph.D. Representative of Graduate Studies	Date
_____	_____
Nilda E. Aponte, Ph.D. Director of Department	Date

Abstract

Discrete zooplankton/micronekton samples from three plankton cruises were collected over a moored Bluewater Broadband ADCP in Mona Passage, west of Puerto Rico to: describe the taxonomic composition, vertical distribution, and diel vertical migrations of the zooplankton/micronekton community, and calibrate ADCP echo intensity data (relative backscatter strength, RBS) versus zooplankton/micronekton biomass and density. A Tucker trawl system (mesh size: 0.2, 0.3, 0.5, 1.0 mm) sampling in vertically stratified step-oblique net tows was used to collect, quantify, and identify zooplankton/micronekton taxa. Three 24-hour net tow stations were occupied over the insonified cone of the 76.8 kHz Acoustic Doppler Current Profiler (ADCP). Echo intensity and current velocity data were acquired from the ADCP. Relative backscatter strength (RBS) time-series contours revealed persistent DVM layers in Mona Passage and La Parguera at depths of 150 and 400 m. Diel vertical migrator (DVM) layers were observed to migrate with maximum vertical velocity ranging from 4 to 12 cm/s. Copepods were the dominant taxon collected in all events, presenting a relative abundance (RA) of approximately 89% of the total zooplankton. The copepod assemblage included *Candacia pachydactila*, *Undinula vulgaris*, *Euchaeta marina*, and *Scolecithrix danae*. Euphausiids, generally strong migrators, were represented by several species of the genus *Stylocheiron*, *Nematoscelis* and *Euphausia*. Statistically significant differences of zooplankton abundance with depth and time of day were detected for several taxonomic groups. Positive linear regressions between RBS and zooplankton/micronekton biomass and densities were statistically significant for several taxonomic groups in the Mona Challenge and Abril La Sierra 2004 cruises. These findings confirmed the existence of a deep scattering layer comprised of zooplankton and micronekton in Caribbean waters, and confirmed the effectiveness of indirect approaches such as the RBS produced by ADCPs to detect such phenomena.

Resumen

Los datos oceanográficos utilizados durante este estudio abarcan tres cruceros de plancton (Mona Challenge, Abril La Sierra 2003 y Abril La Sierra 2004) que muestrearon simultáneamente sobre un perfilador de corrientes (ADCP). Los objetivos fueron: (1) describir la distribución vertical de la comunidad del zooplancton y micronecton, en especial los migradores verticales diurnos (DVM); (2) documentar la migración vertical por medio de series de tiempo y perfiles de desplazamientos verticales; y (3) examinar la relación entre la fuerza de retrodispersión relativa (RBS) y la biomasa y densidad zooplánctica. Se ocuparon tres estaciones de 24 horas sobre el cono de insonificación de un ADCP de 76.8 kHz anclado al fondo marino. El ADCP adquirió datos de velocidad de corrientes e intensidad del eco. Para colectar, cuantificar e identificar las especies del zooplancton y micronecton se utilizó un sistema de redes Tucker (porosidad de la malla: 0.2, 0.3, 0.5 y 1.0 mm) muestreando en arrastres oblicuos-escalonados. Para demostrar la mejor configuración del ADCP en estudios de dinámica de microcapas se añadió y analizó un lanzamiento del ADCP en la pendiente insular de La Parguera. Los contornos de series de tiempo evidenciaron patrones migratorios del zooplancton/micronecton a profundidades entre 150 y 400 m. Las velocidades verticales máximas variaron entre 4 y 12 cm/s. Los copépodos fueron el grupo taxonómico dominante en todos los eventos presentando una abundancia relativa (RA) de aproximadamente 89% del zooplancton total. Algunos posibles migradores identificados incluyen *Candacia pachydactila*, *Undinula vulgaris*, *Euchaeta marina* y *Scolecithrix danae*. Los eufásidos, migradores reconocidos, fueron representados por especies de los géneros *Stylocheiron*, *Nematoscelis* y *Euphausia*. Los análisis de ANOVA mostraron diferencias significativas entre profundidades y tiempos para algunos grupos taxonómicos. Regresiones lineales positivas entre la fuerza de retrodispersión relativa (RBS) y la biomasa y

densidad zooplánctica resultaron estadísticamente significativos ($p < 0.05$) durante los cruceros del Mona Challenge y Abril La Sierra 2004. Estos resultados confirman la existencia de una capa de dispersión profunda (deep scattering layer) producida por componentes zooplánctonicos en aguas del Caribe, y evidencian la efectividad de la señal de RBS producida por un ADCP para detectar dicho fenómeno.

To God, my Family and Hildita my beloved muse,
One Love

Acknowledgements:

I will like to thanks the giant family of Marine Sciences. The administrative staff: Taty, Nilda, Zulma, and Lili, for keeping me updated with my paperwork and deadlines. Plankton Lab team for the acoustic and zooplankton data collection. To my trainers, trainees, and volunteers: Yira, Janneth, Mónica, Arlene, Aury, Rocio, Amaris, Elizabeth, and Taína, in the task of sorting the samples. To the technicians: Bob, Sabater, Rene, Dieppa, Miguel, Felipe, Milton, Alvaro, and Milton Carlo for their support and feedback. My appreciation to Dr. Juan González-Lagoa, Dr. Mark Ohman, and Dr. Annie Townsend for their help in the identification of copepod and euphausiid specimens. I am indebt with my graduate committee members: Drs. Jorge Capella, Jorge Reni Garcia, and Roy Armstrong for their invaluable guidance and teachings. My sponsors during tough times: Maru Mújica, Ricky Camacho, Dr. Jose Papo López, Dr. Jorge Corredor, and Julio Morell. The captains: Cabrilla, Harry, Denny, and their crew for many pleasant times at sea. NOAA – National Marine Fisheries Services for partially funding this study.

Respect

Table of Contents

List of Tables

List of Figures

Introduction

Zooplankton is of fundamental relevance in marine ecosystems as it provides the link between primary producers (phytoplankton) and pelagic consumers, with significant contribution to the nutrient/carbon flux in the ocean. Zooplankton serves as prey for zooplanktivorous fishes, which comprise a numerically dominant assemblage in the outer shelf coral reefs (Garcia et al., 2005), and sustain commercially important pelagic fisheries, such as tunas, jacks, mackerels, runners, billfishes, wahoo, and mahi mahi (Grubbs et al., 2001). Demersal fisheries of deep water snappers (silk and queen) and groupers (misty, yellow-edge, and red hind), are also associated with insular slope habitats (Nelson and Appeldoorn, 1985).

Zooplankton surveys from slope waters off the south and southwest Puerto Rico have been performed by Yoshioka et al. (1985), Pabón-Valentín (2001), González-Figueroa (2002), Rojas (2002) and Ramírez and García (2003). These surveys were performed by traditional net tow samplings encompassing the upper 0 to 100 meter depths, generally at the upper end of the water column, avoiding the bottom because of the equipment loss risks. Thus, the zooplankton closely associated with the benthic habitats of the PR-USVI shelf/slope zone has not been investigated.

During a study of the Atlantic-Caribbean transport across the Mona Passage (Segura, 2000) it was observed that the echo intensity of time-series contours from an 76.8 kHz ADCP showed the presence of a persistent layer of diel vertical migrators (DVM) to depths of 450 m in the central Mona Passage. Recent ichthyoplankton studies over the insular slope of Puerto Rico revealed a similar pattern off Buoy 6 (Abril La Sierra) and La Parguera (off El Hoyo site). Diel vertical migrators (DVM) layers appear to be ubiquitous in pelagic waters, from the continental and insular slopes to the deep abyss, and comprise a wide

variety of marine species. However, echo intensity data from the ADCP provide no information on the biological components associated with acoustic signals.

In theory, 75% of the organisms detected by the 76.8 kHz ADCP should be in the size range from 2 mm to 2 cm (Greenblatt, 1981), comprising most vertical migrant communities of mesozooplankton and macrozooplankton (e.g. large copepods, amphipods and euphausiids), micronekton (e.g. fish larvae and mysids shrimps) and nekton (e.g. small fishes and small squids). Oceanic surveys in the vicinity of southwestern Puerto Rico (Michel and Foyo, 1976) had previously reported that several collected species of copepods, euphausiids and thecosomates exhibited diel vertical behavior. Demersal mesozooplankton and mesopelagic fishes associated with outer reef habitats may be additional components of the DVM community. This study examined zooplankton and micronekton vertical distribution over insular slope habitats of Puerto Rico using traditional plankton net tows and the backscatter signal from an ADCP.

Study Objectives

1. Obtain time-series contours of relative backscatter strength (RBS) from a 76.8 kHz ADCP at Central Mona Passage and the southwestern insular slope of Puerto Rico.

2. Provide preliminary taxonomic and biovolume characterizations of zooplankton/micronekton communities from net samplings within the ADCP insonified cone.

3. Examine the relationship between a 76.8 kHz ADCP backscatter signal and zooplankton biovolume and abundance estimates from samples obtained within the insonified cone.

Literature Review

Diel vertical migration constitutes one of the most important biological processes in the world's oceans. It is considered the largest migration of living organisms in the planet, where every night approximately one billion tons of marine organisms perform a journey to surface waters during the night and descend to the deep during the daytime (Attenborough, 2002). Light is considered the most important cue for diurnal migration (Richards et al., 1996), but an ultimate explanation for diel vertical migration is still unresolved. The most accepted hypothesis for diel vertical migration is visual predator avoidance (Ohman, 1990; De Robertis, 2002). Alternative hypotheses, such as foraging of greater volumes of water, access to near-surface phytoplankton resources, and enhancing metabolic efficiency have also been proposed (Ohman, 1990).

Michel and Foyo (1976) collected several copepods and euphausiids associated with diel vertical behavior in Caribbean Sea waters. In their surveys, planktic copepods observed to migrate diurnally include *Lucicutia flavicornis*, *Rhincalanus cornutus atlantica*, and *Undinula vulgaris*. Migrant euphausiids collected above the thermocline included *Euphausia ternera*, *Thysanopoda acqualis*, and *T. tricuspidata*, while those caught partially below it included *Nematobrachion flexipes*, *Nematoscelis microps/atlantica*, *Thysanopoda monocantha*, and *T. pectinata.* These migrants are relatively large compared to the rest of the zooplankton community, and represent the primary food resource for visual predators, such as zooplanktivorous fishes (De Robertis, 2002).

Vertical and temporal distributions of zooplankton and ichthyoplankton within the surface mixed layer (SML: 0-60m) were examined by González-Figueroa (2002) at a station off the shelf edge of Guayanilla Bay and did not found any differences in abundance. Ramírez (2000) described the vertical distribution of ichthyoplankton, also within the SML, off the shelf edge at La Parguera. Results showed a homogeneous, temporally inconsistent vertical

distribution of fish larvae. Ramírez (2000) suggested that caution should be taken when analyzing the data due to the small sample sizes and the level of taxonomic identification of larval fishes (Family) used may have masked species-specific trends in vertical distribution. Yoshioka et al. (1985) found no significant day/night variation in zooplankton abundance associated with mass vertical migration in oceanic waters south of Puerto Rico.

It should be noted that all former studies collected samples in the upper 60 m (Ramírez, 2000; González-Figueroa, 2002) to 100 m (Yoshioka et. al, 1985), which represents 20 percent or less of the full vertical extent of the water column (depending on strata being sampled). Most importantly, diel vertical migrators (mesozooplankton, macrozooplankton, and nekton) tend to be large and possess the ability to avoid nets. Sameoto et al. (1983) observed that tow speeds of less than three knots decrease catches of euphausiids, an important component of diel vertical migrators (DVM). Most zooplankton sampling in Puerto Rican waters has been performed at tow speeds of less than three knots.

Whereas traditional net samplings have not demonstrated vertical migration by zooplankton or micronekton in Puerto Rican waters, there is conclusive evidence that it occurs in some areas of PR. In the late fifties a study conducted over insular slope waters north of Puerto Rico revealed DVM for the first time (Johnson et al., 1956). They lowered an echo sounder to a depth of 105 fathoms (190 m) and documented a deep scattering layer (DSL) ascending at a rate of fifteen feet per minute. The echo intensity time series observed during the Mona Passage transport study (Segura, 2000) provided the first modern documentation of DVM structures in Puerto Rico.

More recently, ADCPs were employed by Rojas (2002) and Estevez (2005) to examine the spawning, dispersal, and recruitment of two important commercially-exploited fish larvae (*Epinephelus guttatus* and *Lutjanus analis*, respectively) in the insular shelf/slope break of southwestern Puerto Rico. The water velocity profiles obtained from two bottom-mounted ADCPs (76.8 and 300

kHz) were used to estimate pseudo-trajectories of fish eggs and larvae in these studies.

Raw echo intensity data, obtained off the shelf edge at Buoy 6 (Abril La Sierra) and Central Mona Passage as a byproduct from the 76.8 kHz ADCP, revealed higher values during the night. Also, the presence of a persistent DVM structure to 450 meters has been observed at the shelf edge off La Parguera (Capella, personal data; García et al., 2003). The taxonomic identity of scatterers responsible for these higher night values and the persistent DVM structure are unknown.

Acoustics have been widely used as an important tool for localizing fish stocks. Recent studies have confirmed the utility of acoustic instruments to assess zooplankton/micronekton patchiness (microlayers) and their bio-dynamics (Greene et al., 1994). In addition, acoustic technology offers an indirect approach to relate echo data to meaningful biological parameters such as size and numerical density. The acoustic scattering process is a complex function of animal size, shape, orientation, material properties, as well as acoustic frequency (Stanton and Chu, 2000). In order to obtain accurate estimates, the best available representation (model) of the scattering characteristics of the DVM and calibrated acoustical data are required. Greenblatt (1981) studied the types of marine organisms causing backscattering from 87.5 kHz narrow beam sonar. He used three methods to determine the sources of the acoustical scattering: the theoretical, the multiple ping length, and the simultaneous sampling approaches.

In the theoretical approach, the Johnson fluid-sphere scattering model combined with a hypothesized distribution of scatterers was suggested for predicting the percentage of total scattering due to marine organisms of a particular size range. This approach was derived from the idea in respect to the Johnson fluid-sphere formula that, if there are no systematic differences in scattering characteristics of different taxonomic groups of organisms (g and h constant) and for a constant sound frequency (k), the total scattered sound

depends on the size distribution of scatterers. Results showed that at a frequency of 87.5 kHz, 75 % of the scatterers varied in size from 2 mm to 2 cm. This theoretical approach predicted that large zooplankton, fish larvae, small squid, and small fish would be responsible for the scattering.

The multiple ping length approach inferred scatterer abundance from probability distributions of acoustic scattering strength for different insonified volumes. Greenblatt (1981) predicted two changes: (1) an increase in the maximum value of scattering strength with a decrease in ping length, and (2) a decrease in mean scattering strength with decreasing ping lengths. A similar interpretation is that when small volumes are insonified large single targets (fish and squid) will dominate the scattering, when the insonified volume increases smaller scatterers will eventually equal the scattering cross-section of the fish or squid. In the simultaneous sampling approach, he compared the level and pattern of scattering strength calculated from plankton samples using the Johnson fluid-sphere scattering model to the backscatter observed with 87.5 kHz sonar.

The methods of determining reverberation sources yield similar results, but important discrepancies exist. The theoretical approach required no data, but gave the least reliable information because it predicted the same sources of scattering both day and night. The simultaneous sampling approach showed that the sources of scattering change from day to night. An underestimation of scattering strength by net samples in the evening was attributed to net avoidance by midwater fish and squid. Late night scattering levels are explained by increased numbers of euphausiids later at night. Greenblatt (1981) suggested that complicated biological interactions between euphausiids, fish, and squid might be occurring, but concluded that in some instances the 87.5 kHz sonar could be used to quantify accurately the spatial distribution of large zooplankton and small nekton.

Stanton et al. (1996) reviewed acoustic scattering models for zooplankton and supported an alternative idea. They tested three major models: the fluid-like (e.g. shrimp-like animals and salps), the gas-bearing (e.g. siphonophores), and elastic-shelled (e.g. gastropods). They concluded that differences in morphologies of various zooplankton groups could lead to differences in their scattering signatures and therefore, their degree of scattering efficiency. These have a profound impact on the interpretation of acoustic survey data, where changes in species composition within a community and not biomass, could cause changes in acoustic echo levels. The evolution of fluid-like sphere to distorted wave borne approximation (DWBA) models was addresses by Stanton and Chu (2000), but the practical question of this study was which model provides sufficient accuracy for the scientific problem of interest. The focus was on fluid-like zooplankton (i.e. animals that do not support shear waves) with examples specific to euphausiids, shrimps, and copepods. Acoustic scattering predictions were made over a wide range of shape and material property profiles, ranging from simple low-resolution (sphere models) to complex high-resolution (DWBA models) representations of the animals. It was found that for volume scattering strength measurements and as a proxy for biomass estimation the simpler low-resolution (sphere) models could be reliably used.

In addition to acoustic complexity other factors could be influencing acoustic scattering in Puerto Rican and Caribbean waters. Zooplankton and micronekton communities in subtropical oligotrophic oceanic waters are intricate taxonomic assemblages of different species with distinct morphologies and behaviors. Nevertheless, many researchers (Sameoto et al., 1983; Flagg and Smith, 1989; Batchelder et al., 1995; Sindlinger et al., 2005) have successfully used a synoptic approach of nets and acoustics to characterize zooplankton and micronekton assemblages.

Sameoto et al. (1983) characterized two different areas of Canada's Atlantic waters, the Gulf of St. Lawrence and the Nova Scotia shelf/slope break,

using the BIONESS sampler and 120 kHz sounder. They focused on micronekton that could be detected with sounders operating in the range of 30 to 200 kHz. Organisms migrating to surface at night could be separated from other non-migrant scatterers making the signal easier to interpret. The Gulf of St. Lawrence was characterized by homogeneous layers of adult euphausiids populations (*Meganyctiphanes norvergica*, *Thysanoessa raschii*, and *T. inermis*) extending over many kilometers during spring and summer. A contrasting species composition was found at the Nova Scotia study site, where dominant micronekton was comprised by the amphipod *Parathemisto abyssorum*, the euphausiids *M. norvergica* and *T. longicaudata*, a pelagic shrimp *Sergestes arcticus*, and a myctophid fish *Benthosema glaciale*. The Nova Scotia shelf/slope break is described as a frontal boundary zone separating cold coastal waters from warm slope waters. Sameoto et al. (1983) concluded that the 120 kHz sounder was a powerful tool providing valuable information on vertical and horizontal distribution of micronekton. On the other hand, its use for studying complex micronekton community on the Nova Scotia site was limited to obtaining qualitative information on the existence of scattering layers and to document vertical migration.

Flagg and Smith (1989) tested the applicability of a 300 kHz ADCP to estimate zooplankton abundance over New England shelf during springtime. Results showed positive significant correlations between the backscattered signal intensity and total zooplankton volume, cross-sectional area, and dry-weight. The four largest stages of the copepod *Calanus finmarchicus* (mean: 1.27-2.62 mm) plus euphausiid furciliae and adolescents (mean: 3.48-9.39 mm) explained 52-72 % of the total volumes, and 50-73 % of total dry weights. Flagg and Smith (1989) suggested that after calibrating the backscattered signal, an acoustic time-series could be transformed into a biomass time-series. They suggested that since intensities and vertical velocities were obtained by

independent methods within the ADCP, any agreement reassured the reality of time-series contours.

Batchelder et al. (1995) studied temporal and spatial acoustic backscatter estimates of zooplankton biomass using a 153 kHz ADCP during the May 1991 Marine Light-Mixed Layers (MLML) cruises to the North Atlantic. They recalled the importance of sampling fine scales to correctly evaluate the interactions between plankton and their physical/biological environment. Such interactions are difficult if not impossible to resolve with traditional approaches. Relative backscatter was converted to zooplankton biomass estimates using samples collected with a MOCNESS system.

Zooplankton biomass was dominated by *Calanus* copepodites (53 %), *Thysanoessa* developmental life stages (20 %), small copepods (17 %), and large copepods, such as *Euchaeta norvergica* (8 %). They reported a small but consistent diel pattern in the 20 to 250 m depth-integrated backscatter, with highest values during darkness. The nightly oblique zooplankton samples showed increasing densities of possible scatterers (especially *C. finmarchicus*) during middle and late May, soon after the peak of the spring phytoplankton bloom. This increase was mirrored by a comparable increase of the depth-integrated acoustic backscatter, suggesting that seasonal patch dynamics could be inferred by acoustic methods.

Sindlinger et al. (2005) designed a study to measure current velocities and collect backscatter intensity (ABI) data from a 300 kHz ADCP in the northeast Gulf of Mexico. This study sought to compare/contrast spatial and temporal ABI variability related with zooplankton patchiness. They found that ABI in epipelagic waters averaged 3 dB higher at night than during the day suggesting diel vertical migration of zooplankton and/or micronekton. Spatial variability was associated with lower ABI in a warm anti-cyclonic filament and higher ABI in a cyclonic eddy. As these mesoscale features changed location and shape the ABI signal proved to be a useful proxy to follow these changes.

During this study, bongo net tows taken concurrently with ABI measurements provided zooplankton biomass estimates. In theory, the smallest size of zooplankton and micronekton detected by the ADCP would be one quarter of the ADCP wavelength or a size 1.25 mm. The regression of ABI and log of plankton biomass showed that -103 dB corresponded to 9.6 ml/100 m^3 and -98 dB corresponded to 10.5 ml/100 m^3. These data suggest that ABI is sensitive to relatively small changes in wet displacement volume (WDV).

Similar mesoscale features, such as mesoscale eddies and the Orinoco and Amazon river plumes, documented in the Caribbean (Calef and Grice, 1967; Yoshioka, 1985; Corredor et al., 2004) could support higher phytoplankton stocks, increased zooplankton/micronekton biomass, and attract major apex predators (Sindlinger et al., 2005). Pantropical spotted dolphins around Hawaii feed primarily at night on organisms associated with the deep scattering layer as it rises to the surface after dark (Baird et al., 2001). It is possible that large pelagic predators (marlins, mackerels, tunas, and dolphinfish) could be preying on nekton associated with the DVM community and/or on the DVM community itself (Grubbs et al., 2001).

Diel vertical migrators (DVM) play an important role in the nutrient/carbon flux of the ocean, and consequently, in the global geochemical cycles. Diel vertically migrating zooplankton contribute significantly to the dissolved carbon and nutrient export by respiration and excretion of dissolved inorganic carbon and nitrogen, and dissolved organic carbon below the pycnocline. In addition, particulate organic carbon and nitrogen are actively transported when DVM defecates below the mixed layer (Schnetzer and Steinberg, 2002). This active transport by DVM and the passive transport by sinking particles, such as marine snow or fecal pellets from surface waters constitute the two main pathways of the biological pump by which carbon and nutrients are sequestered from the mixed layer to the deep sea.

Materials and Methods

Study Site Description

This study was conducted at several locations on the south and west coasts of Puerto Rico (Fig. 1). The first cruise was to the central Mona Passage during October 2000 (Mona Challenge or MC), the second was off La Parguera shelf (PRG) in 2002, the third and fourth during March 2003 (AS03) and May 2004 (AS04) respectively, were off the shelf at Buoy 6 (Abril La Sierra). The central Mona Passage location had been occupied by Segura (2000) over a two-year period, therefore establishing the persistence of DVM layers. All sites exhibit permanent stratification of water column salinity and temperature, with seasonal vertical migration of the pycnocline. The depth range for the ADCP deployments encompasses four main water masses: the Surface Mixed Layer (SML), or Caribbean Surface Water (CSW) (0-60m), the Subtropical Underwater (SUW) (115-140 m), the 18°, Mode, or Sargasso Sea Water (SSW) (270-320 m), and the upper reaches Tropical Atlantic Central Water (TACW) (450-700 m) as described by Michel and Foyo (1976).

The central Mona Passage station lies on the ridge that defines the sill depth for the Mona Passage, as shown in Fig.1. This ridge acts as a barrier between Atlantic and Caribbean waters, therefore influencing local hydrodynamics and subsequent biological processes. It also influences internal waves (or bores) traveling through this region. The ADCP was bottom mounted on its southern slope approximately six nautical miles southwest from the tip of El Pichincho promontory, north of Mona Island, and roughly halfway between Puerto Rico and the Dominican Republic (Table 1). Bathymetric contour lines run in a west/northwest-east/southeast axis at the site. Tropical oligotrophic oceanic species mostly characterize the zooplankton/micronekton community in Mona Passage.

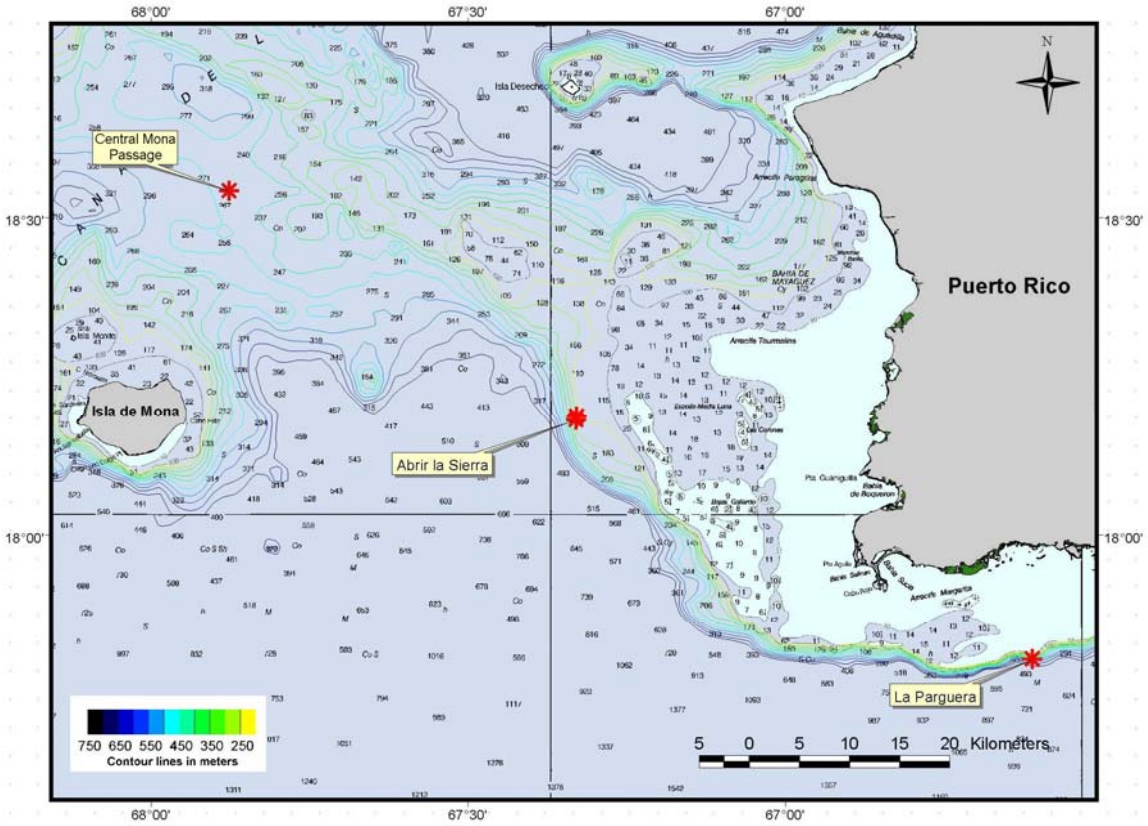

Figure 1. Marine chart of southwestern Puerto Rico. Contour lines in meters. Asterisks (*) indicate ADCP mooring sites.

Table 1. Dates, positions, and depths of ADCP deployments.

Cruises	Dates		Geo-Positions		Bottom	Xducer	6% Xducer
Event	Start	End	Lat (N)	Long (W)	Depth (m)		
MC	24-May-00	11-Oct-00	18° 17.478'	67° 48.155'	470	460	44
PRG	21-Mar-02	08-May-02	17° 52.135'	67° 02.784'	469	462	28
AS03	31-Jan-03	01-May-03	18° 05.087'	67° 28.573'	240	220	13
AS04	26-May-04	9-Aug-04	18° 05.311'	67° 28.534'	243	237	14

The Abril La Sierra and La Parguera sites are part of the southwestern insular shelf of Puerto Rico. During the PRG event the ADCP was bottom mounted in Caribbean Sea slope waters approximately 1 km south from the shelf edge (El Hoyo mooring site, Table 1). Bottom contours at the steep slope are zonal, with a slight southwest to northeast tendency (Capella, personal data; García et al., 2003). Currents at the site are characterized by a low frequency mean west-southwest flow parallel to the shelf and strong tidal flows (Capella, personal data; García et al., 2003). The Abril La Sierra deployments (AS03 and AS04) were located at the same position (Table 1), bottom mounted in slope waters approximately 3 nautical miles off the shelf edge at Buoy 6. Bottom contours run along a meridional axis with a slight northwest to southeast tendency. Water currents at Abril La Sierra and central Mona Passage sites vary significantly, revealing a complex hydrographic regime associated with Atlantic-Caribbean transport and with tidal effects on bathymetric features (Segura, 2000; García et al., 2003). The zooplankton/micronekton communities of La Parguera and Abril La Sierra are comprised of a mixed assemblage of neritic, oceanic, and benthic species associated with the shelf/slope break.

Acoustic Data

An RD Instruments 76.8 kHz Blue Water Broadband ADCP bottom mounted in a taut-wire mooring was used in all surveys. Three deployments from two different locations were coupled with plankton net tows during this study. Each ADCP data set is associated with a specific cruise in which plankton collections and other oceanographic data were obtained. ADCP deployments and retrievals were conducted from the R/V Chapman, the R/V Sultana and/or the R/V Pezmar. DGPS positions and depths of the moorings for all events are listed in Table 1. Most ADCP data were collected as part of ongoing research associated with fish spawning aggregations near shelf-edge zones. Three out of

four (the exception was PRG) ADCP deployments were configured to obtain the most reliable current profiles for assessment of ichthyoplankton pseudo-trajectories. Even though these settings limited the resolution for detecting fine scale processes, vertical migration patterns are visible. ADCP configurations for all deployments are described in Table 2.

A nice feature of the ADCP is that it separates velocity or echo intensity profiles into uniform segments called depth cells or bins. Echo intensity was obtained as part of the ADCP signal conditioning process when calculating the Doppler shift to estimate water velocity. Raw echo intensity was transformed into relative backscatter strength using the formula described by Deines (1999), a working version of the sonar equation where a combination of acoustical terms are replaced by quantities that can be measured in the field. Relative backscatter strength (RBS) refers to the log ratio of the received backscatter signal to the incident acoustic signal when a one-cubic meter (1 m^3) sphere is insonified at a distance of one meter. To calculate the relative backscatter strength of a water parcel several variables need to be known: 1) the power transmitted into the water, 2) the acoustic characteristics of the transducer and the resulting acoustic beam, 3) the power attenuation caused by propagation losses (absorption and beam spreading), and 4) the properties of the receivers

Table 2. ADCP configuration during all deployments.

Cruise name	MC	PRG	AS03	AS04
Bin size	10m (33ft)	5m (16 ft)	5m (16ft)	10m (33ft)
Sampling interval	40 min	6 min	20 min	20 min
Pings per ensemble	15	20	30	60
Time between pings	3 sec	3 sec	3 sec	3 sec
Standard deviation	0.97 cm/sec	2.0 cm/sec	1.1 cm/sec	0.48 cm/sec
Xducer to center of deepest bin	16m (52ft)	9.6m (31ft)	9.6m (31ft)	16m (52ft)

(Deines, 1999). In Deines' algorithm, RBS (Sv) is the calibrated echo intensity corrected for beam spreading and sound absorption, and calculated using variables substituting for specific instrument parameters (Eq-1). A simplified version for Deines algorithm is illustrated in RD Instruments practical primer manual (1996).

$$Sv = C + 10\log_{10}((T_x + 273.16)\,R^2) - L_{DBM} - P_{DBM} + 2\alpha R + K_c\,(E - E_r) \qquad \text{(Eq-1)}$$

where:

Sv is the backscattering strength (dB/4πm)

C is the variable representing the combined parameters (dB)

T_x is the temperature of the transducer (°C)

R is the range along the beam to the transducer (m)

L_{DBM} is $10\log_{10}$ of the transmit pulse length (m)

P_{DBM} is $10\log_{10}$ of the transmit power (Watts)

α is the absorption coefficient of water (dB/m)

K_c is the slope response for the particular receiver (dB/LSB)

E is derived from the Received Signal Strength Indicator (RSSI) output

E_r is the real-time reference level

Relative backscatter strength (RBS) was calculated using values proposed by Deines (1999) and the best approximations available. Since the purpose of this study was to compare relative variations of backscatter for one 76.8 kHz ADCP, absolute measurements were not essential. Lacking ADCP specific calibration parameters, values obtained from the literature (Deines, 1999) for C, T_x, P_{DBM}, α, K_c, and E_r were -163.3 dB, 25°C, 15.4 W, 0.027 dB/m, 0.45 dB/LSB, and 40 counts, respectively. L_{DBM} and therefore, the slant range (R) varied between cruises so independent calculations were done. The RSSI output (E) was the variable of interest which was converted to RBS. The

simplest approach to relate RBS (S_v) to the scatterers in the water is based on the idea that Sv is the total sum of echoes produced by all individual scatterers in the insonified water parcel (Eq-2). This simple idea assumes linearity but in the real scenario other factors increase complexity.

$$Sv = N^*(\sigma_{bs}) \qquad \text{(Eq-2)}$$

where:

Sv is the total backscattering strength (dB/4πm)

N is the total number of scatterers in the insonified volume

σ_{bs} is the backscattering strength for an individual scatterer (dB/4πm)

This principle was used to examine correlations. For RBS vs. zooplankton biovolume and abundance regressions, RBS depth-stratified averages were calculated for each zooplankton net tow interval. RBS time-series were then calculated from the ADCP raw data for all good bins on each ensemble. The first and/or second bins closer to the transducer were excluded from the data analyzed because they were potentially biased by the instrument ring. The last bins corresponding to the 6 % of the transducer depth were removed due to side lobe or surface contamination. Vertical displacements can be assessed and confirmed by two different approaches: examining ADCP's vertical velocity (w) measurements or calculating the rate of displacement from the RBS time-series contours.

Zooplankton Data

Zooplankton samples were taken with a 0.7 m^2 opening-closing Tucker trawl net system equipped with a pressure sensor (Minilog 8-TDR Vemco Limited) and flow meters (MF315 OceanTest Equipment Inc.). In general, samples were collected day and/or night in depth stratified step-oblique tows

encompassing different strata over the insonified zone (Table 3). Profiles of salinity, temperature, σ_t, and chlorophyll-a were obtained at the end of each sampling using a CTD (SBE-25). During the MC cruise, a 0.2 mm mesh size was used in all three nets. Day and night duplicates were collected in step-oblique net tows occupying three strata (0-60 m, 60-120 m, and 120-180 m).

For the cruise AS03, nets were fitted with a larger mesh size (0.3 mm) and a day-triplicate of modified step-oblique tows was obtained (0-20 m, 20-60 m, and 60-100 m). In the cruise AS04 additional changes were done to the sampling protocol. One 1.0 mm net and two 0.5 mm nets were used, and step-oblique net tows were performed. The objective was to compare the fishing efficiency between the 1.0 mm net to the 0.5 mm net in the deep stratum (200-100 m), and differences between strata (200-100 m vs. 100-0 m) for the two 0.5 mm nets. One duplicate during the night and one day replicate were performed during May 26, 2004 at Abril la Sierra (Fig. 24). An additional night replicate was obtained during the ADCP retrieval in August 9, 2004. For the comparative statistical procedures (ANOVA's) testing differences of net efficiency and differences of zooplankton abundance between depths, the May night duplicate and the August night replicate were combined. All replicates (May day replicate, May night duplicate, and August night replicate) were combined for the linear regression analysis of zooplankton biovolume/abundance estimates versus RBS.

Table 3. Zooplankton sampling parameters during MC, AS03, and AS04.

Cruise	Type of Tow	# of Layers	Sample Layers (m)	Mesh size	Day / Night
MC	Step-Oblique	3	Surface (0-60)	0.2 mm	Day / Night
			Mid (60-120)		
			Deep (120-180)		
AS03	Step-Oblique	3	Surface (0-20)	0.3 mm	Day
			Mid (20-60)		
			Deep (60-100)		
AS04	Step-Oblique	2	Surface (0-100)	0.5 / 1.0 mm	Night
			Deep (100-200)		

Zooplankton specimens were fixed in a 5% buffered formalin-seawater solution for taxonomic identification and counting. Each sample was fractioned into several size classes (> 2.0 mm, 2.0 – 1.0 mm, and 1.0 - 0.5 mm). Since smaller mesh size were used in the MC and AS03 cruises, an additional smaller size class was obtained from these cruises (0.5 – 0.2 mm and 0.5 – 0.3 mm, respectively). Sieves were prepared using 3 inch (diameter) PVC tubing 4-5 inches tall with mesh pore 2.0, 1.0, 0.5, 0.3, and 0.2 mm. The sample was gently sieved and rinsed through the different sieves and each fraction was backwashed to a beaker for further analyses.

Biovolume (settling volume in ml/l) estimates were determined for each size class using one-liter Inhoff cones. The fractioned sample was poured into the cone and left to settle for 24 hours. After biovolumes estimates were obtained, zooplankton groups were identified to general taxonomic groups and counted. Zooplankton abundance was reported as number (#) of individuals per 100 m^3. For the regression analysis the space sampled by the net was coupled with the ADCP insonified layer. ANOVA procedures were used for all cruises to examine spatial/temporal differences in biovolume estimates and zooplankton groups within each size class. Each size class of the zooplankton was first analyzed as an individual taxonomic group.

In addition, zooplankton was lumped into four different groups: total zooplankton, major zooplankton, shrimp-like zooplankton, and elastic zooplankton. The shrimp-like group consisted of amphipods, brachyurans, carideans, euphausiids, mysids, sergestids, and unidentified shrimps; the elastic group composed by cephalopods, gastropods, fish larvae, ostracods, and siphonophores; and the major zooplankton group comprised by copepods and chaetognaths. Statistical analysis was redone in all four groups to test differences between depths (AS03 and AS04), day and night (MC), and / or net efficiency (AS04). Regressions of RBS depth-stratified averages vs. biovolumes

and RBS depth-stratified averages vs. abundance estimates of taxonomic groups were calculated for each size class. Qualitatively, euphausiids and copepods were identified to species level using the *Euphausiids of the World Ocean* manual (Brinton et al., 1999) and the expertise of Dr. Annie Johnston (SIO) and Dr. Juan González-Lagoa (UPRM).

Results

Acoustic Data

The sharpest vertical and temporal resolution of acoustic RBS time-series was observed during the PRG event, where microlayers associated with diel vertical migration and reverse migration are evident (Fig. 2). The coarsest RBS time-series resolution was observed during the MC cruise, but a vertical migration pattern still evident (Fig. 3). AS03 and AS04 cruises exhibited an intermediate resolution (Figs. 4-6). All ADCP deployments revealed a pattern of higher RBS during the night at the lower portion of the mixed layer and in most events clear vertical migratory features. Maximum vertical velocity profiles corroborated active vertical displacement (Figs. 7-10). The PRG and MC deployments evidenced sharp diel vertical migration from a deep layer at roughly 400 m during dusk and dawn. In all DVM cycles, the descent at dawn was the most abrupt vertical displacement.

The MC DVM layer descended at 12 cm/s and ascended at 5 cm/s (Fig. 7). Maximum downward and upward velocities of 6 cm/s and 4 cm/s, respectively were observed during AS03, but the diel cycle was not apparent (Fig. 8). AS04 showed maximum downward and upward velocities of 9 cm/s and 5 cm/s, respectively (Fig. 9 and Fig. 10). During August 8, 2004, the maximum sunrise vertical displacement was upward at a speed of 5 cm/s (Fig. 10) suggesting that reverse diel vertical migrators (RDVM) were present. RDVM behavior is the counter mechanism of DVM; an ascent during the day and a descent during the night (Ohman, 1990).

During the PRG event, vertical velocity profiles (Fig.11) most clearly support the migrating behavior observed in the time-series contour (Fig. 2). The PRG time-series contour (Fig. 2) exhibits DVM and alternatively, RDVM. The maximum descent and ascent velocities of DVM were 12 cm/s and 10 cm/s,

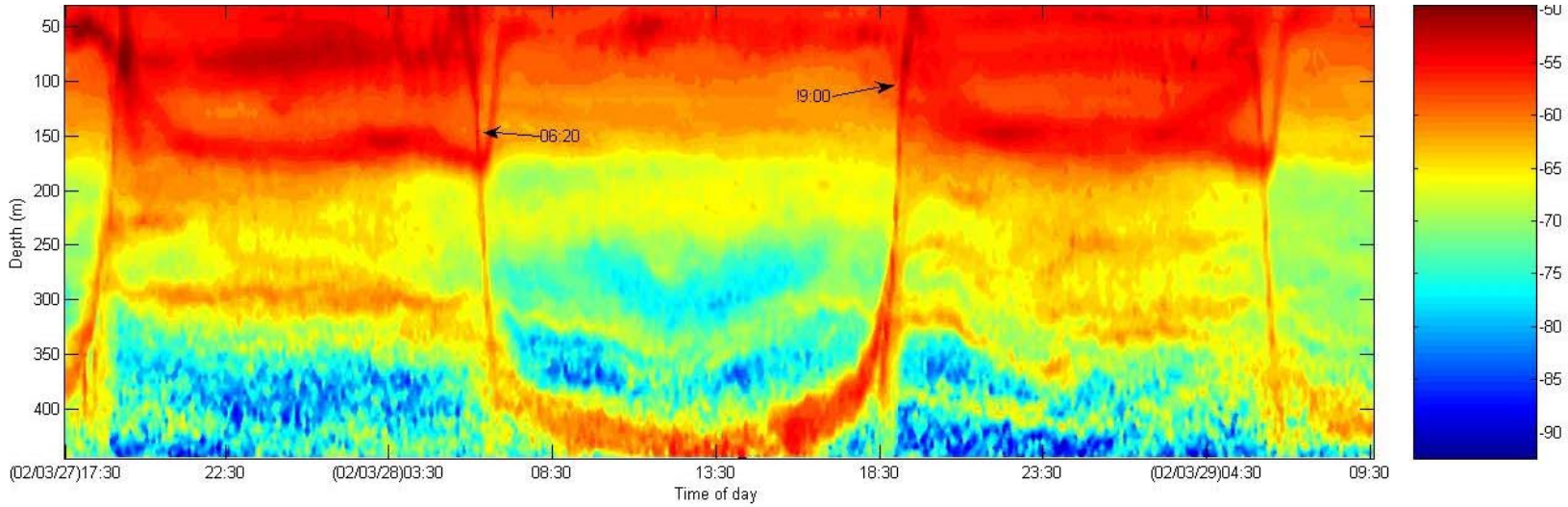

Figure 2. La Parguera (PRG) deployment relative backscatter strength (RBS-dB) time-series, March 2002 (bin size = 5 m, pings/ensemble = 20, and sampling interval = 6 min).

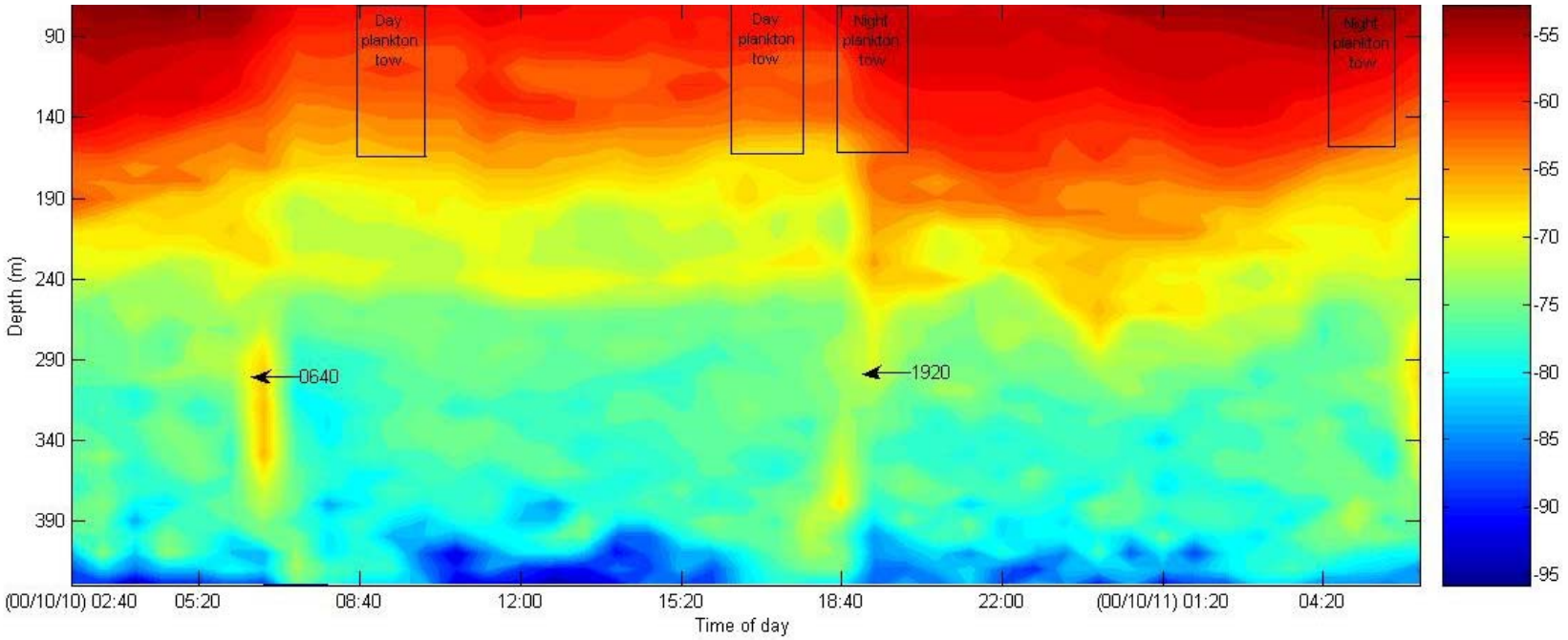

Figure 3. Central Mona Passage (MC) deployment relative backscatter strength (RBS-dB) time-series, October 2000 (bin size = 10 m, pings/ensemble = 15, and sampling interval = 40 min).

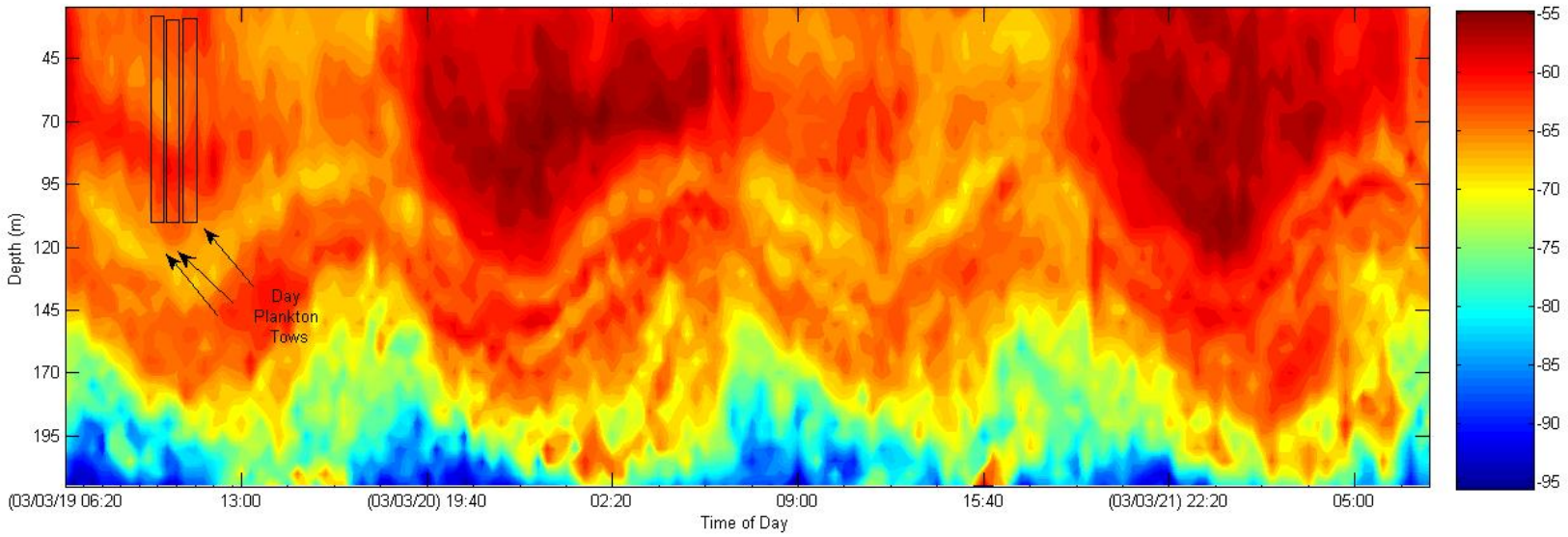

Figure 4. Abril La Sierra (AS03) deployment relative backscatter strength (RBS-dB) time-Series, March 2003 (bin size = 5 m, pings/ensemble = 30, and sampling interval = 20 min).

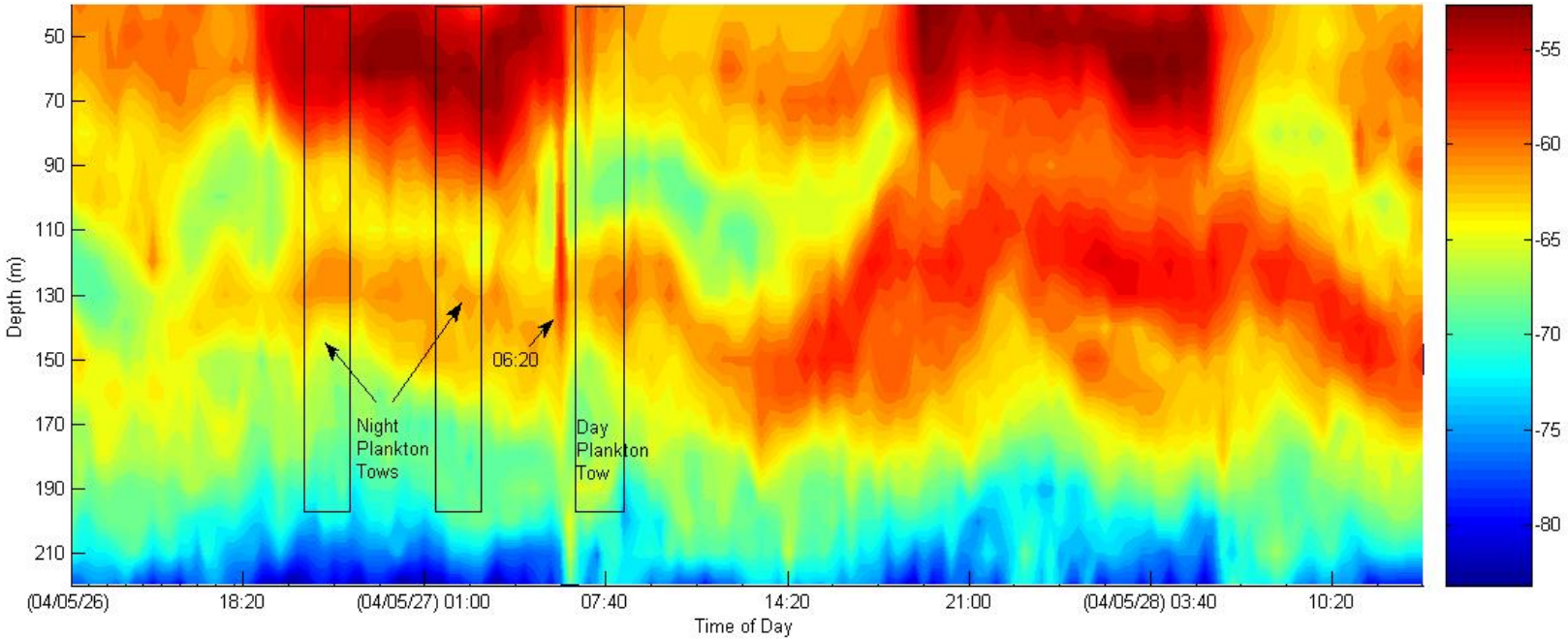

Figure 5. Abril La Sierra (AS04) deployment relative backscatter strength (RBS-dB) time-series, May 2004 (bin size = 10 m, pings/ensemble = 40, and sampling interval = 20 min).

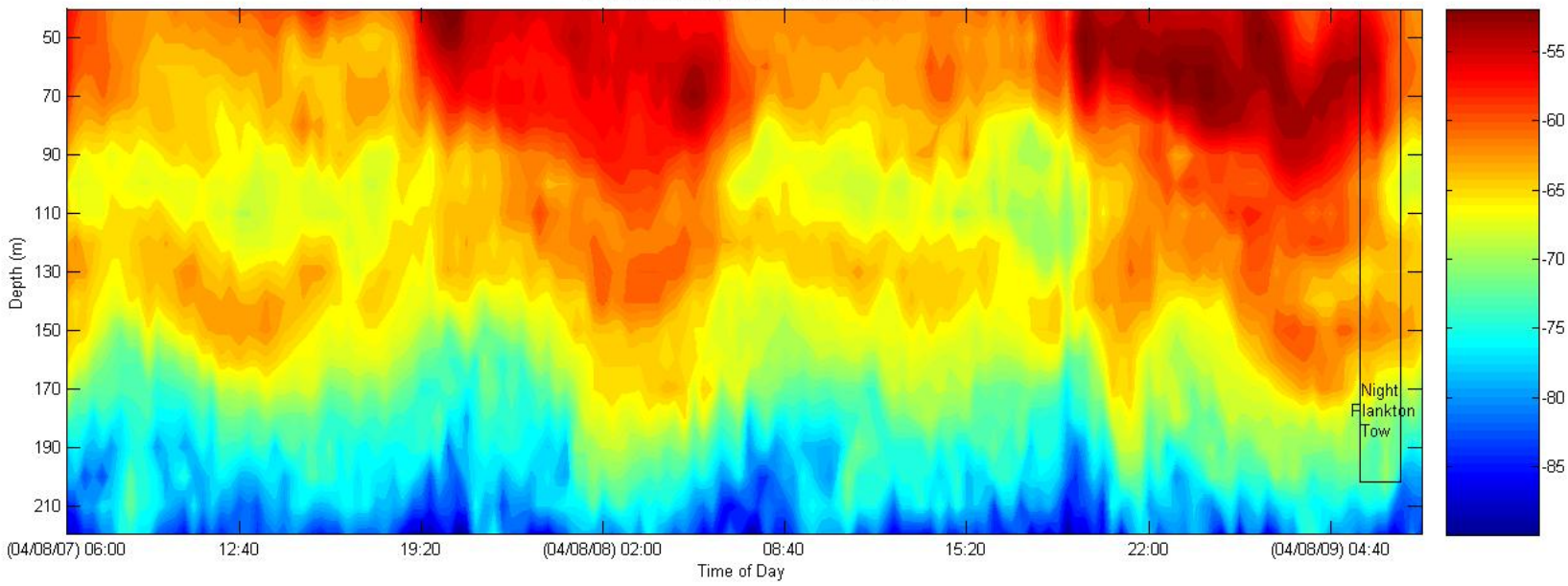

Figure 6. Abril La Sierra (AS04) deployment relative backscatter strength (RBS-dB) time-series, August, 2004 (bin size = 10 m, pings/ensemble = 40, and sampling interval = 20 min).

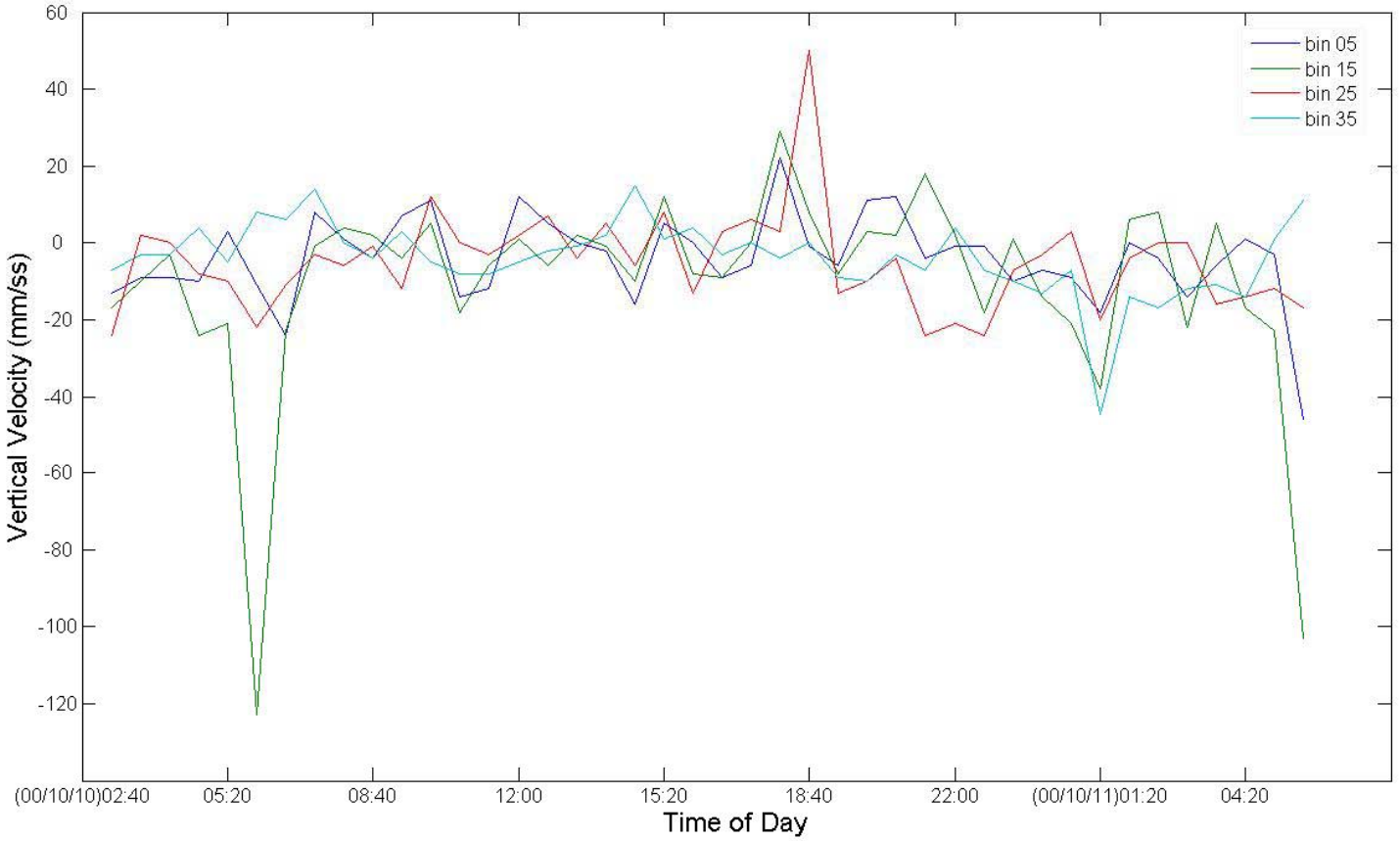

Figure 7. Maximum velocity time-series during the MC event.

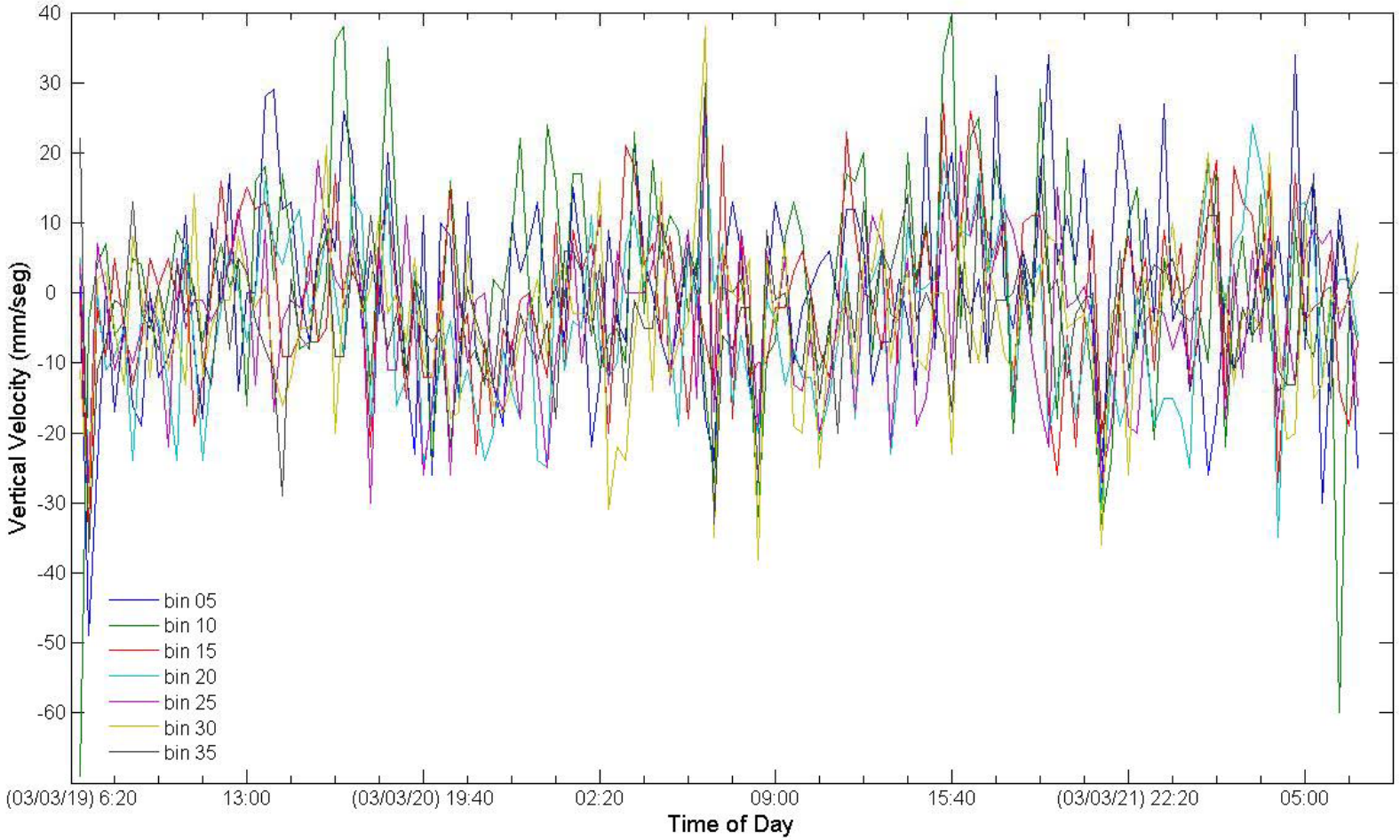

Figure 8. Maximum velocity time-series during the AS03 event.

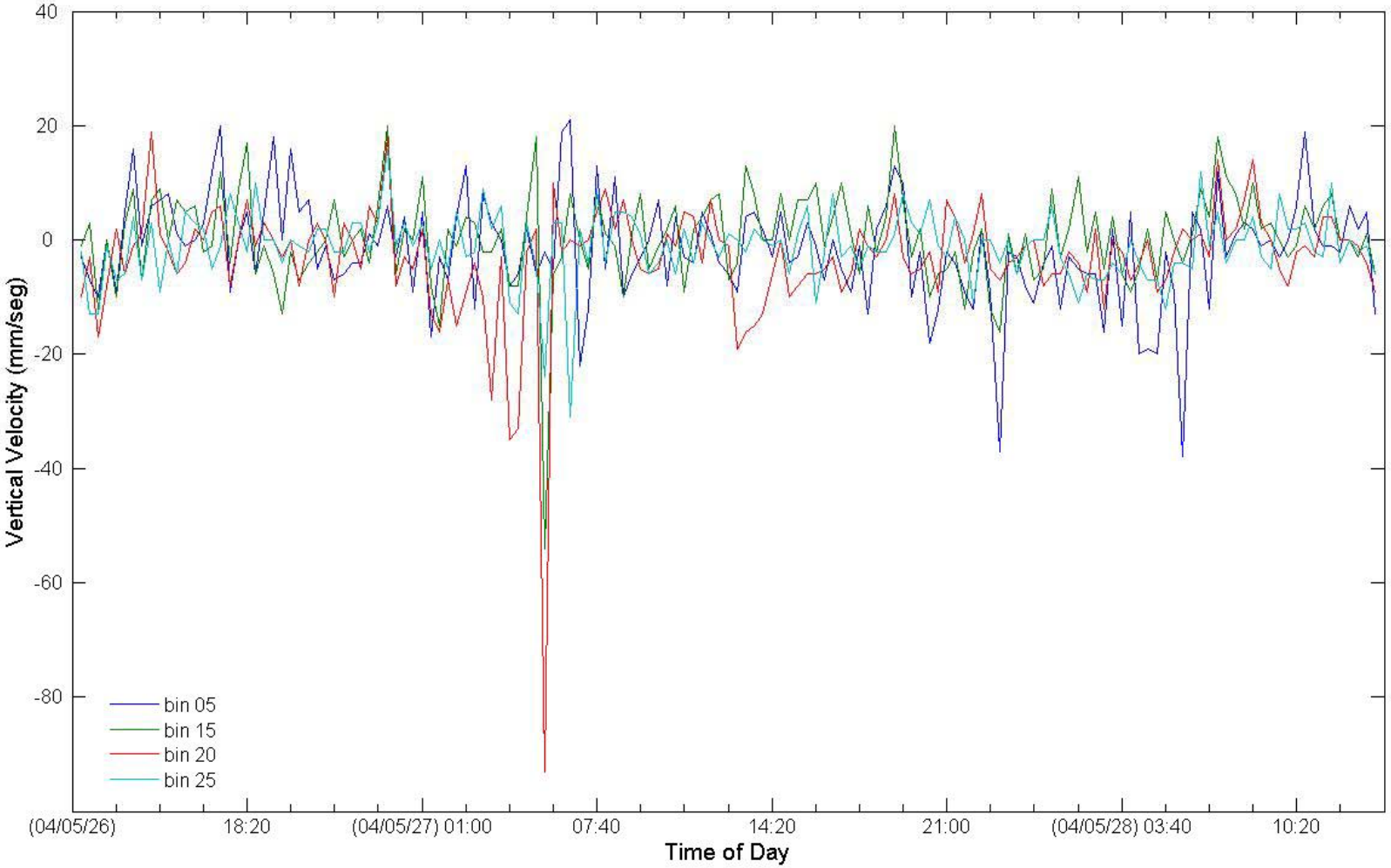

Figure 9. Maximum velocity time-series during the AS04 event (May 2004).

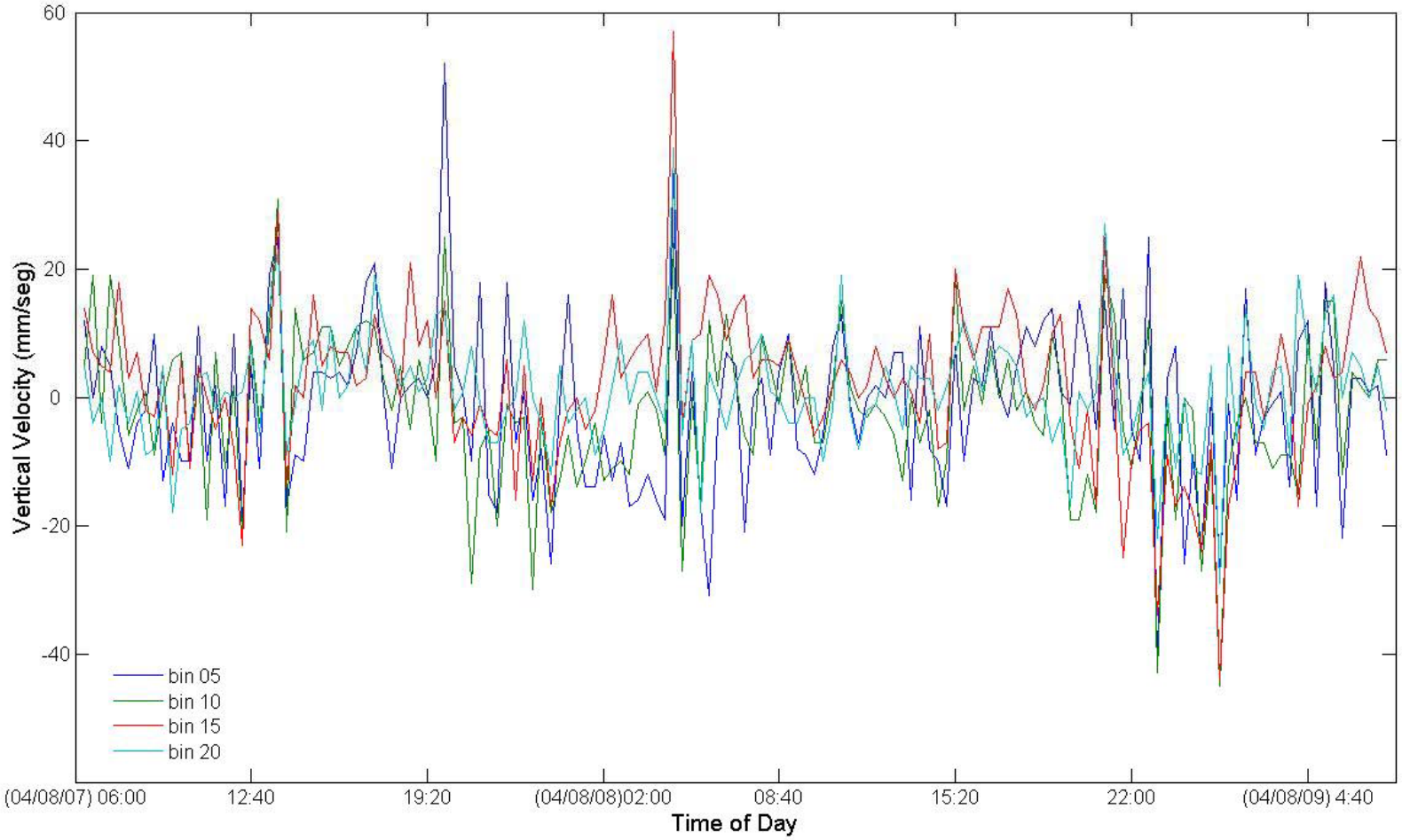

Figure 10. Maximum velocity time-series during the AS04 event (August 2004).

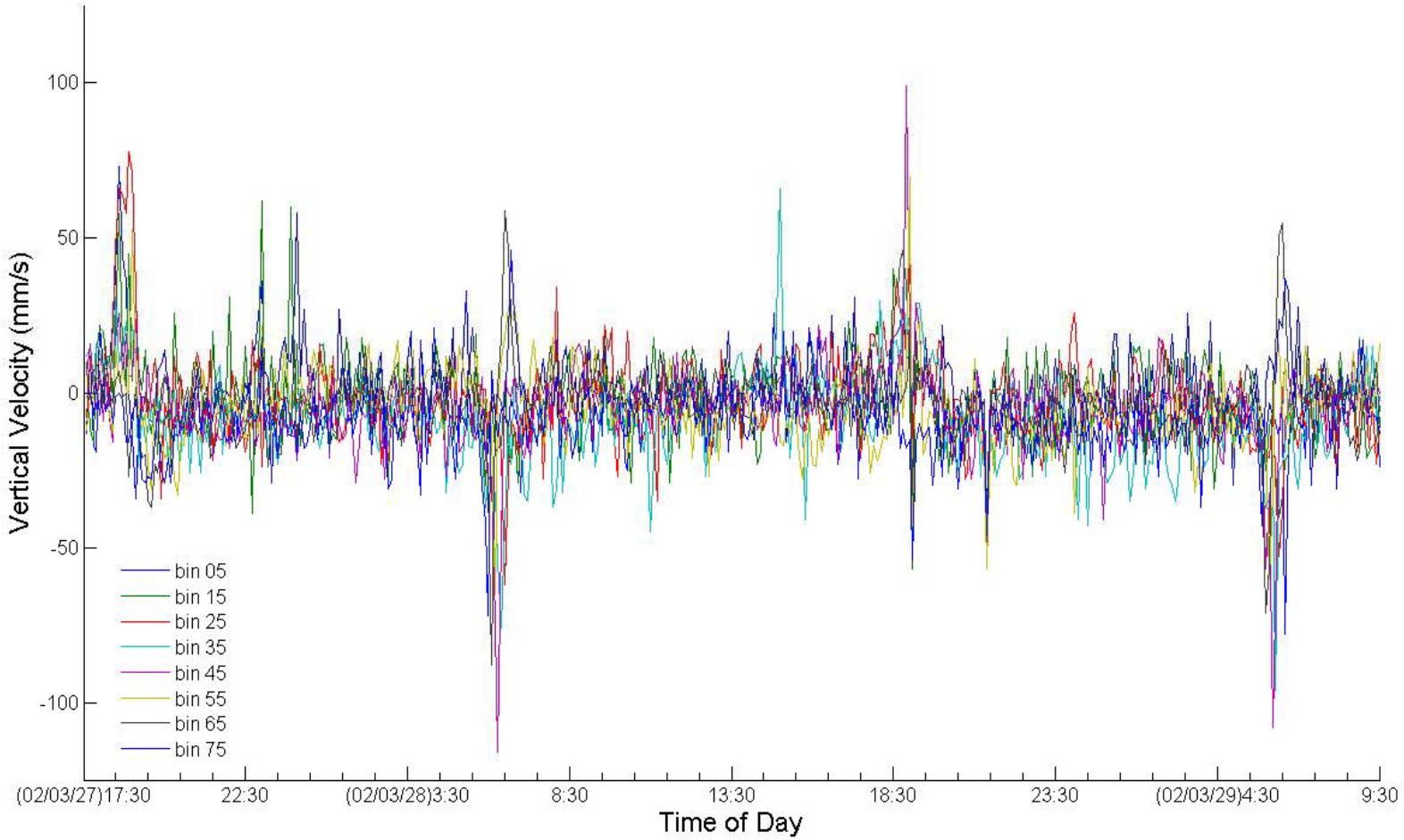

Figure 11. Maximum velocity time-series during the PRG deployment.

respectively (Fig.11). In addition, RDVM are suggested in the PRG time-series contour where a diffuse layer has an abrupt ascent during sunrise but a gradual descent during the afternoon (Fig.2). Vertical velocity profiles support the existence of the RDVM layer with a maximum upward velocity of 6 cm/s during their sunrise ascent (Fig. 11).

Zooplankton Abundance Estimates and RBS Regressions

Calanoid copepods were the dominant taxonomic group of the zooplankton community during all events (Tables 4-6). The largest and most common oceanic copepods collected within the 2 mm to 0.5 mm size range were adult stages of *Candacia pachydactyla*, *Undinula vulgaris*, *Scolecithrix danae*, and *Euchaeta marina* (Fig. 12). Smaller common copepods collected within the 0.5 mm to 0.2 mm size range included *Oithona plumifera*, *Miracia efferata*, and *Corycaeus amazonicus* (Fig. 12).

Two main patterns of zooplankton distribution were observed during the MC event; statistically significant differences between depth layers (Tables 4 and 7) with higher densities at the surface (Figs. 13 and 14), and statistically significant differences of zooplankton abundance between day and night (Figs. 13 and 14; Tables 4 and 7). Most zooplankton groups showed higher densities during the day than at night at the 60-120 m (mid) layer (two-factor ANOVA; $p \leq 0.05$). The variation of zooplankton abundance between day and night at the 120-180 m depth layer was not statistically significant (ANOVA; $p > 0.05$). Copepods were the main taxonomic component of the total zooplankton assemblage accounting for 89% of the total individuals collected in samples (Fig. 15 and Table 4). The smallest sized copepods (0.5-0.2 mm) accounted for 76% of the total collection. Siphonophores were more abundant during the night at the deep layer, but at the mid layer behaved similarly to the other zooplankton groups (Fig. 16). The shrimp-like group, an assemblage comprising possible

Table 4. Zooplankton groups mean and relative abundance (RA) during the MC cruise.

Variable (ind/100m^3)	Day						Night					
	Deep	**RA**	**Mid**	**RA**	**Surf**	**RA**	**Deep**	**RA**	**Mid**	**RA**	**Surf**	**RA**
All zoo group 2.0 mm	20	0.23	60	0.23	103	0.21	22	0.18	7	0.06	115	0.27
All zoo group 1.0 mm	157	1.81	1638	6.18	1607	3.21	353	3.00	172	1.50	2160	5.13
All zoo group 0.5 mm	887	10.22	4057	15.30	6967	13.94	1662	14.13	1663	14.52	5945	14.12
All zoo group 0.2 mm	7610	87.76	20758	78.29	41315	82.64	9723	82.69	9610	83.92	33887	80.48
All zoo group total	8672	(-)	26513	(-)	49992	(-)	11758	(-)	11452	(-)	42107	(-)
Amphipods 2.0 mm	0	0	0	0	0	0	0	0	0	0	0	0
Amphipods 1.0 mm	2	0.02	8	0.03	12	0.02	7	0.06	5	0.04	8	0.02
Amphipods 0.5 mm	2	0.02	5	0.02	20	0.04	12	0.10	2	0.01	8	0.02
Amphipods 0.2 mm	5	0.06	0	0	8	0.02	7	0.06	0	0	0	0
Amphipods Total	8	0.10	13	0.05	40	0.08	25	0.21	7	0.06	17	0.04
Brachyurans 2.0 mm	0	0	0	0	2	0	0	0	0	0	0	0
Brachyurans 1.0 mm	0	0	2	0.01	13	0.03	2	0.01	2	0.01	8	0.02
Brachyurans 0.5 mm	2	0.02	10	0.04	0	0	8	0.07	5	0.04	3	0.01
Brachyurans 0.2 mm	0	0	0	0	0	0	0	0	0	0	0	0
Brachyurans Total	2	0.02	10	0.04	13	0.03	10	0.09	7	0.06	20	0.05
Carideans 2.0 mm	2	0.02	2	0.01	2	0	0	0	0	0	2	0
Carideans 1.0 mm	2	0.02	10	0.04	13	0.03	3	0.03	3	0.03	18	0.04
Carideans 0.5 mm	2	0.02	5	0.02	28	0.06	3	0.03	2	0.01	7	0.02
Carideans 0.2 mm	0	0	0	0	0	0	0	0	0	0	0	0
Carideans Total	6	0.06	17	0.06	43	0.09	7	0.06	5	0.04	27	0.06
Cephalopods 2.0 mm	0	0	0	0	0	0	0	0	0	0	0	0
Cephalopods 1.0 mm	0	0	0	0	0	0	0	0	0	0	2	0
Cephalopods 0.5 mm	2	0.02	0	0	0	0	0	0	0	0	0	0
Cephalopods 0.2 mm	0	0	0	0	0	0	0	0	0	0	0	0
Cephalopods Total	2	0.02	0	0	0	0	0	0	0	0	2	0

Table 4. Cont.

Variable (ind/100m^3)	Day						Night					
	Deep	**RA**	**Mid**	**RA**	**Surf**	**RA**	**Deep**	**RA**	**Mid**	**RA**	**Surf**	**RA**
Chaetognaths 2.0 mm	12	0.13	42	0.16	82	0.16	12	0.10	2	0.01	78	0.19
Chaetognaths 1.0 mm	22	0.25	228	0.86	317	0.63	57	0.48	12	0.10	713	1.69
Chaetognaths 0.5 mm	67	0.77	242	0.91	638	1.28	137	1.16	63	0.55	497	1.18
Chaetognaths 0.2 mm	18	0.21	87	0.33	202	0.40	70	0.60	13	0.12	30	0.07
Chaetognaths total	118	1.36	598	2.26	1240	2.48	273	2.32	90	0.79	1318	3.13
Copepods 2.0 mm	2	0.02	3	0.01	3	0.01	3	0.03	2	0.01	5	0.01
Copepods 1.0 mm	105	1.21	1258	4.75	965	1.93	235	2.00	120	1.05	1167	2.77
Copepods 0.5 mm	625	7.21	3215	12.13	5205	10.41	1178	10.02	1367	11.93	4273	10.15
Copepods 0.2 mm	6772	78.09	18870	71.17	39327	78.67	8707	74.05	9260	80.86	31350	74.45
Copepods total	7503	86.53	23348	88.06	45500	91.02	10123	86.09	10747	93.84	36795	87.39
Elastic group 2.0 mm	2	0.02	2	0.01	2	0	2	0.01	0	0	3	0.01
Elastic group 1.0 mm	7	0.08	13	0.05	7	0.01	10	0.09	5	0.04	25	0.06
Elastic group 0.5 mm	117	1.35	295	1.11	193	0.39	187	1.59	155	1.35	238	0.57
Elastic group 0.2 mm	677	7.80	1027	3.87	383	0.77	642	5.46	312	2.72	303	0.72
Elastic group total	798	9.21	840	3.17	1337	2.67	472	4.01	585	5.11	570	1.35
Euphausiids 2.0 mm	0	0	3	0.01	0	0	3	0.03	2	0.01	7	0.02
Euphausiids 1.0 mm	7	0.08	20	0.08	2	0	15	0.13	8	0.07	30	0.07
Euphausiids 0.5 mm	0	0	13	0.05	8	0.02	5	0.04	0	0	5	0.01
Euphausiids 0.2 mm	0	0	0	0	0	0	0	0	0	0	0	0
Euphausiids total	7	0.08	37	0.14	10	0.02	23	0.20	10	0.09	40	0.09
Plankton eggs 2.0 mm	0	0	0	0	0	0	0	0	0	0	0	0
Plankton eggs 1.0 mm	0	0	0	0	0	0	0	0	0	0	0	0
Plankton eggs 0.5 mm	0	0	0	0	0	0	0	0	0	0	0	0
Plankton eggs 0.2 mm	1135	13.09	4277	16.13	10998	22.00	1387	11.79	1002	8.75	6530	15.51
Plankton eggs total	1135	13.09	4277	16.13	10998	22.00	1387	11.79	1002	8.75	6530	15.51

Table 4. Cont.

Variable (ind/100m^3)	Day						Night					
	Deep	RA	Mid	RA	Surf	RA	Deep	RA	Mid	RA	Surf	RA
Fish larvae 2.0 mm	0	0	2	0.01	2	0	2	0.01	0	0	2	0
Fish larvae 1.0 mm	2	0.02	12	0.04	5	0.01	5	0.04	2	0.01	22	0.05
Fish larvae 0.5 mm	3	0.04	25	0.09	20	0.04	13	0.11	2	0.01	58	0.14
Fish larvae 0.2 mm	3	0.04	13	0.05	28	0.06	0	0	32	0.28	0	0
Fish larvae total	8	0.10	53	0.20	57	0.11	20	0.17	33	0.29	80	0.19
Gastropods 2.0 mm	0	0	0	0	0	0	0	0	0	0	0	0
Gastropods 1.0 mm	0	0	0	0	0	0	0	0	2	0.01	0	0
Gastropods 0.5 mm	3	0.04	5	0.02	12	0.02	12	0.10	33	0.29	8	0.02
Gastropods 0.2 mm	0	0	0	0	52	0.10	13	0.11	0	0	0	0
Gastropods total	3	0.04	5	0.02	63	0.13	25	0.21	33	0.29	8	0.02
Larvaceans 2.0 mm	0	0	0	0	0	0	0	0	0	0	0	0
Larvaceans 1.0 mm	0	0	0	0	8	0.02	5	0.04	0	0	7	0.02
Larvaceans 0.5 mm	8	0.10	97	0.36	368	0.74	10	0.09	0	0	370	0.88
Larvaceans 0.2 mm	118	1.36	753	2.84	1338	2.68	253	2.15	3	0.03	2103	5.00
Larvaceans total	127	1.46	850	3.21	1717	3.43	267	2.27	3	0.03	2480	5.89
Major Zoo 2.0 mm	17	0.19	52	0.19	95	0.19	15	0.13	5	0.04	102	0.24
Major Zoo 1.0 mm	135	1.56	1543	5.82	1403	2.81	307	2.61	145	1.27	2005	4.76
Major Zoo 0.5 mm	710	8.19	3610	13.62	6355	12.71	1377	11.71	1440	12.57	5342	12.69
Major Zoo 0.2 mm	6912	79.70	19718	74.37	40917	81.85	9043	76.91	9282	81.05	33507	79.58
Major Zoo Total	7773	89.64	24923	94.00	48772	97.56	10742	91.35	10872	94.94	40953	97.26
Ostracods 2.0 mm	0	0	0	0	0	0	0	0	0	0	0	0
Ostracods 1.0 mm	2	0.02	0	0	0	0	3	0.03	2	0.01	0	0
Ostracods 0.5 mm	100	1.15	238	0.90	142	0.28	148	1.26	117	1.02	143	0.34
Ostracods 0.2 mm	673	7.76	1007	3.80	297	0.59	620	5.27	280	2.45	303	0.72
Ostracods total	775	8.94	1245	4.70	438	0.88	772	6.56	398	3.48	447	1.06

Table 4. Cont.

Variable (ind/100m^3)	Day						Night					
	Deep	RA	Mid	RA	Surf	RA	Deep	RA	Mid	RA	Surf	RA
Polychaetes 2.0 mm	0	0	0	0	0	0	0	0	0	0	0	0
Polychaetes 1.0 mm	2	0.02	2	0.01	0	0	2	0.01	0	0	3	0.01
Polychaetes 0.5 mm	10	0.12	27	0.10	20	0.04	13	0.11	5	0.04	28	0.07
Polychaetes 0.2 mm	0	0	7	0.03	7	0.01	8	0.07	0	0	0	0
Polychaetes total	12	0.13	35	0.13	28	0.06	23	0.20	5	0.04	33	0.08
Sergestids 2.0 mm	0	0	0	0	0	0	0	0	0	0	0	0
Sergestids 1.0 mm	0	0	8	0.03	2	0	2	0.01	0	0	3	0.01
Sergestids 0.5 mm	0	0	5	0.02	28	0.06	3	0.03	0	0	8	0.02
Sergestids 0.2 mm	0	0	0	0	0	0	0	0	0	0	0	0
Sergestids total	0	0	15	0.06	30	0.06	5	0.04	0	0	13	0.03
Shrimp-like group 2.0 mm	2	0.02	7	0.03	7	0.01	5	0.04	2	0.01	12	0.03
Shrimp-like group 1.0 mm	17	0.19	82	0.31	197	0.39	35	0.30	22	0.19	128	0.30
Shrimp-like group 0.5 mm	60	0.69	153	0.58	418	0.84	98	0.84	67	0.58	367	0.87
Shrimp-like group 0.2 mm	23	0.27	13	0.05	15	0.03	38	0.33	17	0.15	77	0.18
Shrimp-like group total	100	1.15	255	0.96	635	1.27	178	1.52	107	0.93	583	1.39
Shrimps 2.0 mm	0	0	0	0	0	0	0	0	0	0	0	0
Shrimps 1.0 mm	5	0.06	35	0.13	152	0.30	7	0.06	3	0.03	57	0.13
Shrimps 0.5 mm	55	0.63	115	0.43	277	0.55	67	0.57	58	0.51	335	0.80
Shrimps 0.2 mm	18	0.21	13	0.05	7	0.01	33	0.28	17	0.15	68	0.16
Shrimps total	78	0.90	163	0.62	493	0.99	107	0.91	78	0.68	460	1.09
Siphonophores 2.0 mm	2	0.02	7	0.03	12	0.02	2	0.01	2	0.01	18	0.04
Siphonophores 1.0 mm	8	0.10	57	0.21	112	0.22	12	0.10	13	0.12	118	0.28
Siphonophores 0.5 mm	12	0.13	57	0.21	142	0.28	52	0.44	12	0.10	200	0.47
Siphonophores 0.2 mm	3	0.04	7	0.03	50	0.10	12	0.10	5	0.04	23	0.06
Siphonophores total	25	0.29	127	0.48	317	0.63	77	0.65	32	0.28	360	0.85

Table 4. Cont

Variable (ind/100m^3)	Day						Night					
	Deep	**RA**	**Mid**	**RA**	**Surf**	**RA**	**Deep**	**RA**	**Mid**	**RA**	**Surf**	**RA**
Stomatopods 2.0 mm	0	0	2	0.01	2	0	0	0	0	0	2	0
Stomatopods 1.0 mm	0	0	0	0	3	0.01	0	0	0	0	3	0.01
Stomatopods 0.5 mm	0	0	0	0	0	0	0	0	0	0	0	0
Stomatopods 0.2 mm	0	0	0	0	0	0	0	0	0	0	0	0
Stomatopods total	0	0	2	0.01	5	0.01	0	0	0	0	5	0.01

Table 5. Mean and relative abundance (RA) of zooplankton groups during the AS03 cruise.

Variable (ind/100 m^3)	Day mean					
	0-20 m	**RA**	**20-60 m**	**RA**	**60-100 m**	**RA**
All zooplankton group 2.0 mm	25	0.75	40	0.67	28	0.63
All zooplankton group 1.0 mm	493	14.71	330	5.54	128	2.85
All zooplankton group 0.5 mm	920	27.44	1288	21.61	770	17.07
All zooplankton group 0.3 mm	1915	57.11	4305	72.21	3585	79.49
All zooplankton group total	3353	(-)	5962	(-)	4510	(-)
Amphipods 2.0 mm	0	0	0	0	0	0
Amphipods 1.0 mm	2	0.05	3	0.06	2	0.04
Amphipods 0.5 mm	7	0.20	8	0.14	8	0.18
Amphipods 0.3 mm	2	0.05	2	0.03	7	0.15
Amphipods total	10	0.30	15	0.25	17	0.37
Anomurans 2.0 mm	0	0	0	0	0	0
Anomurans 1.0 mm	0	0	0	0	0	0
Anomurans 0.5 mm	0	0	2	0.03	5	0.11
Anomurans 0.3 mm	0	0	0	0	2	0.04
Anomurans total	0	0	2	0.03	7	0.15
Brachyurans 2.0 mm	0	0	0	0	0	0
Brachyurans 1.0 mm	2	0.05	2	0.03	2	0.04
Brachyurans 0.5 mm	7	0.20	5	0.08	12	0.26
Brachyurans 0.3 mm	2	0.05	2	0.03	10	0.22
Brachyurans total	10	0.30	8	0.14	23	0.52
Carideans 2.0 mm	0	0	0	0	0	0
Carideans 1.0 mm	5	0.15	5	0.08	3	0.07

Table 5. Cont.

Variable (ind/100 m^3)	Day mean					
	0-20 m	**RA**	**20-60 m**	**RA**	**60-100 m**	**RA**
Carideans 0.5 mm	10	0.30	5	0.08	2	0.04
Carideans 0.3 mm	0	0	2	0.03	0	0
Carideans total	15	0.45	13	0.22	7	0.15
Cephalopods 2.0 mm	0	0	0	0	0	0
Cephalopods 1.0 mm	0	0	0	0	0	0
Cephalopods 0.5 mm	0	0	0	0	0	0
Cephalopods 0.3 mm	0	0	0	0	0	0
Cephalopods total	0	0	0	0	0	0
Chaetognaths 2.0 mm	17	0.50	28	0.48	22	0.48
Chaetognaths 1.0 mm	75	2.24	92	1.54	52	1.15
Chaetognaths 0.5 mm	52	1.54	72	1.20	47	1.03
Chaetognaths 0.3 mm	3	0.10	10	0.17	13	0.30
Chaetognaths total	147	4.37	203	3.41	133	2.96
Copepods 2.0 mm	2	0.05	0	0	2	0.04
Copepods 1.0 mm	368	10.98	182	3.05	42	0.92
Copepods 0.5 mm	765	22.81	1055	17.70	568	12.60
Copepods 0.3 mm	1108	33.05	3183	53.40	2138	47.41
Copepods total	2245	66.95	4420	74.14	2750	60.98
Plankton eggs 2.0 mm	0	0	0	0	0	0
Plankton eggs 1.0 mm	0	0	0	0	0	0
Plankton eggs 0.5 mm	0	0	0	0	0	0
Plankton eggs 0.3 mm	778	23.21	1017	17.05	1227	27.20

Table 5. Cont.

Variable (ind/100 m^3)	Day mean					
	0-20 m	RA	20-60 m	RA	60-100 m	RA
Plankton eggs total	778	23.21	1017	17.05	1227	27.20
Elastic group 2.0 mm	0	0	0	0	0	0
Elastic group 1.0 mm	2	0.05	2	0.03	2	0.04
Elastic group 0.5 mm	8	0.25	8	0.14	3	0.07
Elastic group 0.3 mm	3	0.10	7	0.11	17	0.37
Elastic group total	12	0.35	17	0.28	22	0.48
Euphausiids 2.0 mm	0	0	0	0	0	0
Euphausiids 1.0 mm	12	0.35	5	0.08	0	0
Euphausiids 0.5 mm	8	0.25	7	0.11	0	0
Euphausiids 0.3 mm	0	0	0	0	0	0
Euphausiids total	20	0.60	12	0.20	2	0.04
Larvaceans 2.0 mm	0	0	0	0	0	0
Larvaceans 1.0 mm	0	0	0	0	0	0
Larvaceans 0.5 mm	0	0	12	0.20	23	0.52
Larvaceans 0.3 mm	5	0.15	37	0.62	138	3.07
Larvaceans total	5	0.15	48	0.81	162	3.58
Major group 2.0 mm	23	0.70	40	0.67	28	0.63
Major group 1.0 mm	465	13.87	307	5.14	112	2.48
Major group 0.5 mm	843	25.15	1210	20.30	682	15.11
Major group 0.3 mm	1902	56.71	4267	71.57	3532	78.31
Major group total	3233	96.42	5823	97.68	4353	96.53
Ostracods 2.0 mm	0	0	0	0	0	0

Table 5. Cont.

Variable (ind/100 m^3)	Day mean					
	0-20 m	**RA**	**20-60 m**	**RA**	**60-100 m**	**RA**
Ostracods 1.0 mm	0	0	0	0	0	0
Ostracods 0.5 mm	5	0.15	7	0.11	2	0.04
Ostracods 0.3 mm	2	0.05	7	0.11	17	0.37
Ostracods total	7	0.20	14	0.22	18	0.41
Polychaetes 2.0 mm	0	0	0	0	0	0
Polychaetes 1.0 mm	2	0.05	2	0.03	2	0.04
Polychaetes 0.5 mm	2	0.05	2	0.03	2	0.04
Polychaetes 0.3 mm	0	0	0	0	0	0
Polychaetes total	3	0.10	3	0.06	3	0.08
Sergestids 2.0 mm	0	0	0	0	0	0
Sergestids 1.0 mm	2	0.05	2	0.03	2	0.04
Sergestids 0.5 mm	7	0.20	5	0.08	3	0.07
Sergestids 0.3 mm	0	0	0	0	0	0
Sergestids total	9	0.25	7	0.11	5	0.11
Shrimp-like group 2.0 mm	0	0	2	0.03	0	0
Shrimp-like group 1.0 mm	27	0.80	22	0.36	15	0.33
Shrimp-like group 0.5 mm	68	2.04	68	1.15	83	1.85
Shrimp-like group 0.3 mm	10	0.30	30	0.50	37	0.81
Shrimp-like group total	107	3.18	123	2.07	137	3.03
Shrimps 2.0 mm	0	0	0	0	0	0
Shrimps 1.0 mm	5	0.15	3	0.06	5	0.11
Shrimps 0.5 mm	28	0.84	35	0.59	52	1.15

Table 5. Cont.

Variable (ind/100 m^3)	Day mean					
	0-20 m	**RA**	**20-60 m**	**RA**	**60-100 m**	**RA**
Shrimps 0.3 mm	7	0.20	23	0.39	20	0.44
Shrimps total	40	1.19	62	1.03	77	1.70
Siphonophores 2.0 mm	5	0.15	10	0.17	5	0.11
Siphonophores 1.0 mm	22	0.65	32	0.53	20	0.44
Siphonophores 0.5 mm	28	0.84	72	1.20	43	0.96
Siphonophores 0.3 mm	5	0.15	18	0.31	15	0.33
Siphonophores total	58	1.74	132	2.21	83	1.85
Stomatopods 2.0 mm	0	0	0	0	0	0
Stomatopods 1.0 mm	2	0.05	2	0.03	2	0.04
Stomatopods 0.5 mm	0	0	2	0.03	0	0
Stomatopods 0.3 mm	0	0	0	0	0	0
Stomatopods total	2	0.05	4	0.06	2	0.04

Table 6. Mean and relative abundance (RA) of zooplankton groups during the AS04 cruise.

Variable (ind/100 m^3)	Mean		
	1.0 mm mesh 100-200 m (RA)	**0.5 mm mesh 100-200 m (RA)**	**0.5 mm mesh 0-100 m (RA)**
All zoo group 2.0 mm	14 ((29.86)	19 (2.01)	104 (3.89)
All zoo group 1.0 mm	34 (70.14)	179 (18.55)	1339 (50.28)
All zoo group 0.5 mm	-	765 (79.47)	1220 (45.83)
All zoo group total	48 (-)	963 (-)	2663 (-)
Amphipods 2.0 mm	1 (2.08)	0 (0)	1 (0.03)
Amphipods 1.0 mm	5 (10.42)	8 (0.87)	35 (1.31)
Amphipods 0.5 mm	-	13 (1.38)	26 (0.96)
Amphipods total	6 (12.50)	22 (2.25)	61 (2.30)
Anomurans 2.0 mm	0 (0)	0 (0)	1 (0.03)
Anomurans 1.0 mm	0 (0)	1 (0.10)	1 (0.05)
Anomurans 0.5 mm	-	0 (0)	0 (0)
Anomurans total	0 (0)	1 (0.14)	2 (0.08)
Brachyurans 2.0 mm	0 (0)	0 (0)	1 (0.03)
Brachyurans 1.0 mm	1 (2.78)	1 (0.14)	7 (0.28)
Brachyurans 0.5 mm	-	28 (2.87)	8 (0.31)
Brachyurans total	1 (2.78)	29 (3.01)	16 (0.61)
Carideans 2.0 mm	1 (1.39)	3 (0.35)	3 (0.11)
Carideans 1.0 mm	2 (4.17)	9 (0.93)	12 (0.44)
Carideans 0.5 mm	-	15 (1.56)	11 (0.41)
Carideans total	3 (5.56)	27 (2.84)	26 (0.96)
Cephalopods 2.0 mm	0 (0)	0 (0.03)	0 (0.01)

Table 6. Cont.

Variable (ind/100 m^3)	Mean		
	1.0 mm mesh 100-200 m (RA)	**0.5 mm mesh 100-200 m (RA)**	**0.5 mm mesh 0-100 m (RA)**
Cephalopods 1.0 mm	0 (0)	0 (0)	2 (0.06)
Cephalopods 0.5 mm	-	0 (0)	3 (0.13)
Cephalopods total	0 (0)	0 (0.03)	5 (0.20)
Chaetognaths 2.0 mm	3 (6.25)	3 (0.28)	53 (1.98)
Chaetognaths 1.0 mm	5 (9.72)	10 (1.04)	195 (7.32)
Chaetognaths 0.5 mm	-	85 (8.79)	183 (6.87)
Chaetognaths total	8 (15.97)	97 (10.11)	431 (16.17)
Copepods 2.0 mm	0 (0.69)	0 (0.03)	15 (0.56)
Copepods 1.0 mm	3 (6.25)	47 (4.85)	653 (24.52)
Copepods 0.5 mm	-	283 (29.39)	732 (27.50)
Copepods total	3 (6.94)	330 (34.27)	1400 (52.58)
Elastic group 2.0 mm	2 (4.17)	2 (0.17)	28 (1.06)
Elastic group 1.0 mm	6 (12.50)	9 (0.97)	109 (4.09)
Elastic group 0.5 mm	-	284 (29.46)	208 (7.81)
Elastic group total	8 (16.67)	295 (30.60)	345 (12.97)
Euphausiids 2.0 mm	7 (15.28)	11 (1.14)	2 (0.09)
Euphausiids 1.0 mm	11 (23.61)	92 (9.52)	317 (11.92)
Euphausiids 0.5 mm	-	56 (5.82)	17 (0.64)
Euphausiids total	19 (38.89)	159 (16.48)	337 (12.64)
Fish larvae 2.0 mm	0 (0)	1 (0.10)	4 (0.14)
Fish larvae 1.0 mm	0 (0)	1 (0.14)	14 (0.51)
Fish larvae 0.5 mm	-	8 (0.87)	12 (0.44)

Table 6. Cont.

Variable (ind/100 m^3)	Mean		
	1.0 mm mesh 100-200 m (RA)	**0.5 mm mesh 100-200 m (RA)**	**0.5 mm mesh 0-100 m (RA)**
Fish larvae total	0 (0)	11 (1.11)	29 (1.09)
Gastropods 2.0 mm	0 (0)	0 (0)	0 (0)
Gastropods 1.0 mm	0 (0)	0 (0)	3 (0.10)
Gastropods 0.5 mm	-	9 (0.93)	14 (0.53)
Gastropods total	0 (0)	9 (0.93)	17 (0.64)
Major zoo group 2.0 mm	3 (6.94)	3 (0.31)	68 (2.54)
Major zoo group 1.0 mm	8 (15.97)	57 (5.88)	848 (31.84)
Major zoo group 0.5 mm	-	368 (38.18)	915 (34.37)
Major zoo group total	11 (22.92)	427 (44.38)	1831 (68.76)
Mysids 2.0 mm	0 (0)	0 (0)	0 (0)
Mysids 1.0 mm	0 (0)	0 (0)	0 (0)
Mysids 0.5 mm	-	0 (0)	4 (0.14)
Mysids total	0 (0)	0 (0)	4 (0.14)
Ostracods 2.0 mm	0 (0)	0 (0)	0 (0)
Ostracods 1.0 mm	1 (1.39)	4 (0.42)	1 (0.03)
Ostracods 0.5 mm	-	161 (16.72)	3 (0.11)
Ostracods total	1 (1.39)	165 (17.13)	4 (0.14)
Sergestids 2.0 mm	0 (0)	0 (0)	0 (0)
Sergestids 1.0 mm	0 (0)	0 (0)	1 (0.05)
Sergestids 0.5 mm	-	0 (0)	12 (0.46)
Sergestids total	0 (0)	0 (0)	13 (0.53)
Shrimp-like group 2.0 mm	9 (18.75)	15 (1.52)	8 (0.29)

Table 6. Cont.

Variable (ind/100 m^3)	Mean		
	1.0 mm mesh 100-200 m (RA)	**0.5 mm mesh 100-200 m (RA)**	**0.5 mm mesh 0-100 m (RA)**
Shrimp-like group 1.0 mm	20 (41.67)	113 (11.70)	382 (14.34)
Shrimp-like group 0.5 mm	-	114 (11.84)	97 (3.64)
Shrimp-like group total	29 (60.42)	241 (25.06)	487 (18.28)
Shrimps 2.0 mm	0 (0)	0 (0)	0 (0)
Shrimps 1.0 mm	0 (0)	1 (0.14)	8 (0.29)
Shrimps 0.5 mm	-	2 (0.17)	19 (0.71)
Shrimps total	0 (0)	3 (0.31)	27 (1.00)
Siphonophores 2.0 mm	2 (4.17)	0 (0)	24 (0.90)
Siphonophores 1.0 mm	5 (9.72)	4 (0.42)	90 (3.39)
Siphonophores 0.5 mm	0 (0)	105 (10.94)	176 (6.61)
Siphonophores total	7 (13.89)	110 (11.39)	290 (10.90)

Table 7. One-way Analysis of Variance (ANOVA) procedures testing differences of zooplankton abundance between day and night samplings at various depth strata (deep 120-180; mid 60-120; surf 0-60) during the MC cruise. The "X" determines significant contrast ($p \leq 0.05$).

Variable	DAY vs. NIGHT					
	Deep	**Mid**	**Surf**	**Deep + Mid**	**Mid + Surf**	**All strata**
All Zoo 2.0 mm		X		X	X	X
All Zoo 1.0 mm		X			X	
All Zoo 0.2 mm		X			X	
All Zoo total		X			X	
Major Zoo 2.0 mm		X		X	X	X
Major Zoo 1.0 mm		X			X	
Major Zoo 0.2 mm		X			X	
Major Zoo total		X			X	
Chaetognaths 1.0 mm		X		X	X	
Chaetognaths 0.5 mm		X			X	
Chaetognaths total		X			X	
Copepods 1.0 mm		X			X	
Copepods 0.2 mm		X				
Copepods total		X			X	
Fish Larvae 0.5 mm		X	X	X	X	
Siphonophores 0.5 mm	X	X			X	
Siphonophores total	X	X				

Plate 1. *Candacia pachydactyla*
(size > 0.5 mm)

Plate 2. *Scolecithrix danae*
(size > 0.5 mm)

Plate 3. *Euchaeta marina*
(size > 0.5 mm)

Plate 4. *Miracia efferata*
(size < 0.3 mm)

Plate 5. *Corycaeus amazonicus*
(size < 0.3 mm)

Figure 12. Digital photographs of several common copepods collected during all the zooplankton cruises.

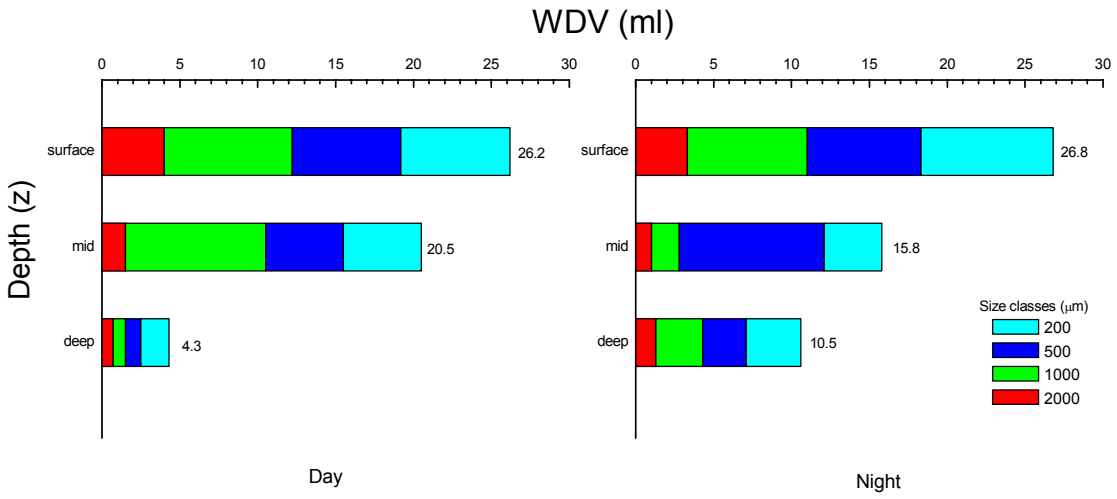

Figure 13. Total zooplankton abundance and vertical distribution during the MC cruise.

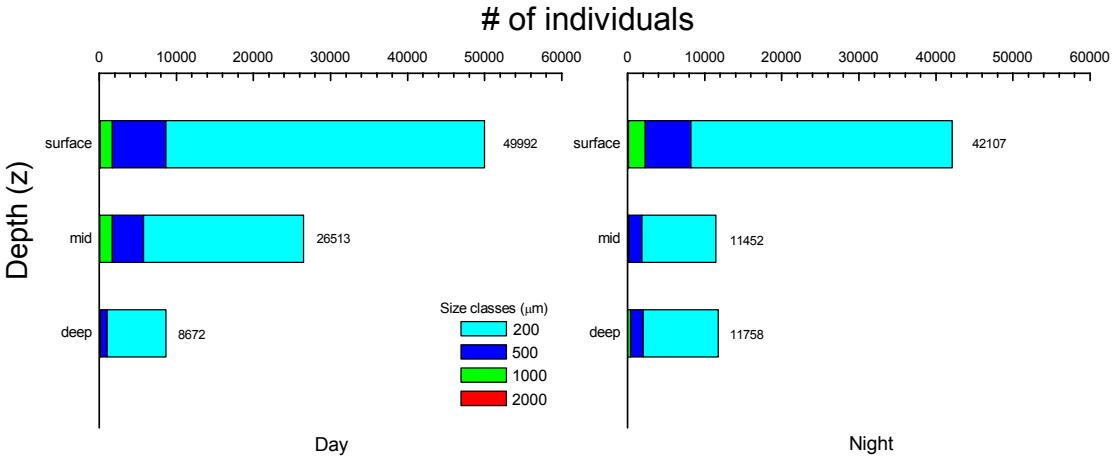

Figure 14. Biovolume vertical distribution during the MC cruise.

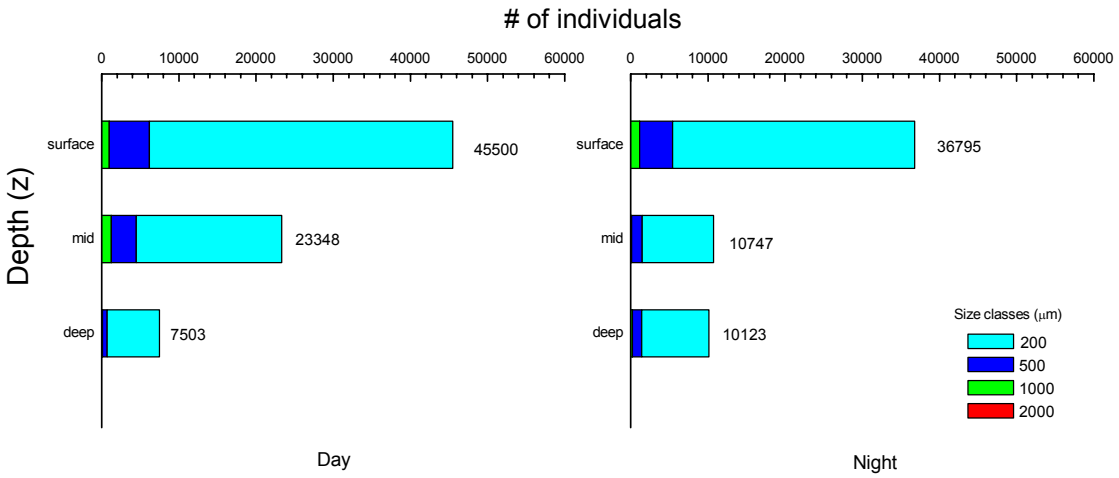

Figure 15. Abundance and vertical distribution of copepods during the MC cruise.

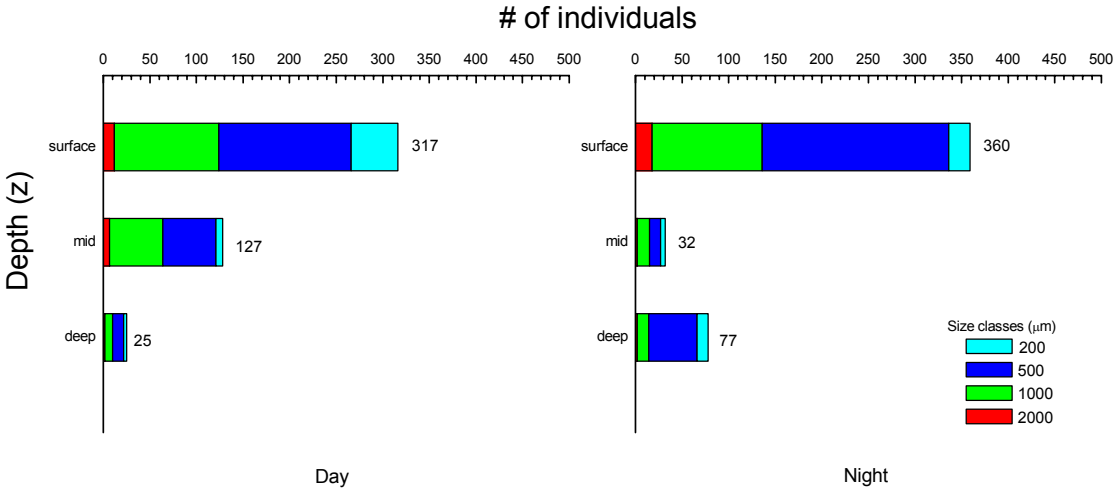

Figure 16. Abundance and vertical distribution of siphonophores during the MC cruise.

migrants, accounted for less than 1% of the zooplankton community. Euphausiids identified within this group include *Stylocheiron abbreviatum*, *S. elongatum*, *S. carinatum*, *S. affine*, *Euphausia gibba*, *E. gibboides*, and *E. mutica* (Fig. 17).

A positive linear relationship was found between RBS and zooplankton biovolume/abundance estimates during the MC event (Table 9; Figs. 20 and 21). The relationship implies that an increment in RBS of 1 dB corresponds to increments of approximately 0.15-0.4 ml of biovolume (size class 0.2-0.5 mm; r^2 = 0.83) and 1,000-6,000 copepods (all size copepods; r^2 = 0.82) per 60 m^3. Difference of zooplankton abundance and biovolume between depth layers were statistically significant during the AS03 cruise (ANOVA; $p \leq 0.05$) for some taxonomic groups (Table 5 and 8). Most of the variability associated with zooplankton vertical distribution during this cruise was explained by the fluctuations in abundance by the 0.3-0.5mm, 0.5-1.0 mm, and 1-2 mm zooplankton size classes, exhibiting distinctive behaviors (Fig. 19). Organisms in the size range of 0.3-1.0 mm were more abundant below depths of 20 m (surface layer) with peak abundance at the mid layer (20-60 m). Organisms in the 1.0-2.0 mm size range were more abundant in the upper 60 m (surface and mid layers), but peaked in abundance at the mid layer (20-60 m).

The total biovolume distribution positively correlated (r^2 = 0.87) with total zooplankton, evidencing peak abundance at the mid layer (Fig. 19). Copepods, plankton eggs, and chaetognaths constituting 67%, 22.5% and 3.6% of the total zooplankton respectively, were the main components of the zooplankton/micronekton assemblage. Identified euphausiids included *Euphausia tenera*, *Thysanoessa tricuspidata*, and *Stylocheiron carinatum* (Fig. 17). Regression models during the AS03 event evidenced a relatively weak negative trend for some groups (Table 10).

The specific objectives of the AS04 cruise were to compare fishing efficiency between two mesh sizes and to compare differences of zooplankton

Table 8. One-way Analysis of Variance (ANOVA) procedures testing differences between depth layers during the AS03 cruise. The "X" corresponds to statistically significant differences ($p \leq 0.05$).

Variable	20-60 vs. 60-100 m	0-20 vs. 20-60 m	0-20 vs. 60-100 m
Biovolume 2.0 mm	X		
Biovolume 1.0 mm		X	X
Biovolume 0.3 mm	X	X	
Biovolume total		X	
All zooplankton group 1.0 mm		X	X
All zooplankton group 0.3 mm	X		
Shrimp-like group 0.3 mm	X		
Major zooplankton group 1.0 mm		X	X
Major zooplankton group 0.3 mm	X		
Amphipods 1.0 mm		X	
Amphipods 0.3 mm			X
Copepods 1.0 mm		X	X
Copepods 0.3 mm	X		
Copepods total	X		
Ostracods 0.3 mm			X
Siphonophores 2.0 mm	X		
Siphonophores total	X		

Table 9. Zooplankton abundance and biovolume regression models (logx+1) vs. relative backscatter strength (RBS) during the MC cruise.

Variable	Regression Model	R^2 Value	T-Value	P-value
Biovolume 0.2 mm	0.03x + 2.32	0.83	6.71	0.0001
All zoo group 0.2 mm	0.05x + 7.17	0.82	6.08	0.0003
All zoo group total	0.05x + 7.32	0.82	5.96	0.0003
Shrimp-like group 0.5 mm	0.06x + 5.67	0.83	6.32	0.0002
Major zoo group 0.2 mm	0.06x + 7.32	0.82	6.11	0.0003
Major zoo group total	0.06x + 7.47	0.82	6.04	0.0003
Copepods 0.2 mm	0.05x + 7.25	0.82	5.99	0.0003
Copepods total	0.05x + 7.36	0.82	5.96	0.0003
Ostracods 1.0 mm	-0.03x – 1.76	0.59	-3.77	0.0037
Unidentifed shrimps 0.5 mm	0.06x + 5.67	0.80	5.58	0.0005

Table 10. Zooplankton abundance/biovolume regression models (logx+1) vs. relative backscatter strength (RBS) during the AS03 cruise.

Variable	Regression Model	R^2 Value	T-Value	P-Value
Biovolume 1.0 mm	-0.02x – 1.02	0.58	-3.09	0.0177
Biovolume total	-0.02x – 0.83	0.47	-2.48	0.0419
All zoo group 0.3 mm	-0.04x + 0.99	0.56	-3.01	0.0195
Shrimp-like group 0.3 mm	-0.05x – 1.86	0.55	-2.91	0.0228
Major zoo group 0.3 mm	-0.04x + 0.99	0.56	-2.99	0.0202
Copepods 0.3 mm	-0.04x + 0.33	0.60	-3.27	0.0137
Ostracods 0.3 mm	-0.05x – 2.65	0.47	-2.51	0.0403
Unidentified shrimps 0.3 mm	-0.04x – 1.69	0.50	-2.66	0.0326

Plate 6. *Stylocheiron abbreviatum*
(size ~ 1.0 cm)

Plate 7. *Stylocheiron carinatum*
(size ~ 1.0 cm)

Plate 8. *Euphausia tenera*
(size 7.0 mm)

Plate 9. *Thysonopoda tricuspidata*
(size 1.0 cm)

Figure 17. Digital photographs (I) of several euphausiids collected during the zooplankton cruises.

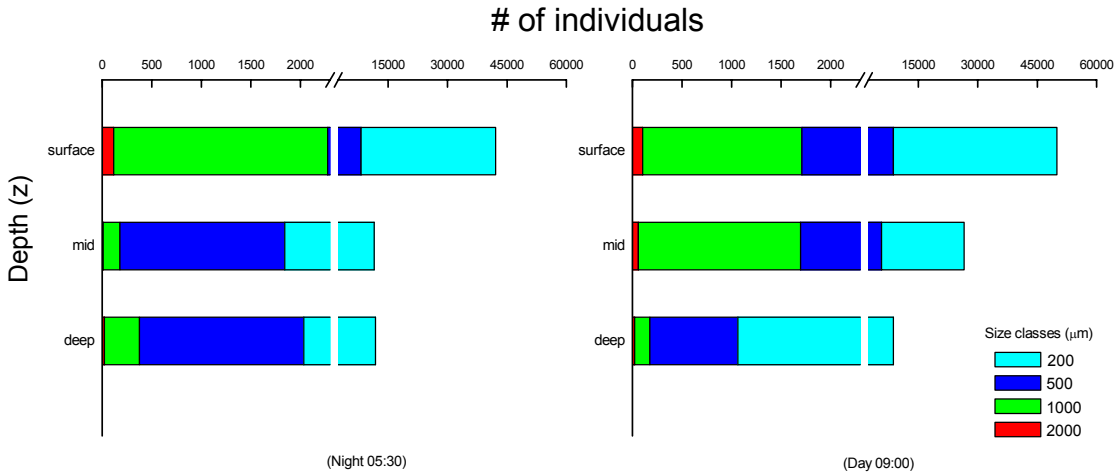

Figure 18. Replicates abundance difference of total zooplankton larger than 1.0 mm at the deep layer reflected at the MC RBS time-series.

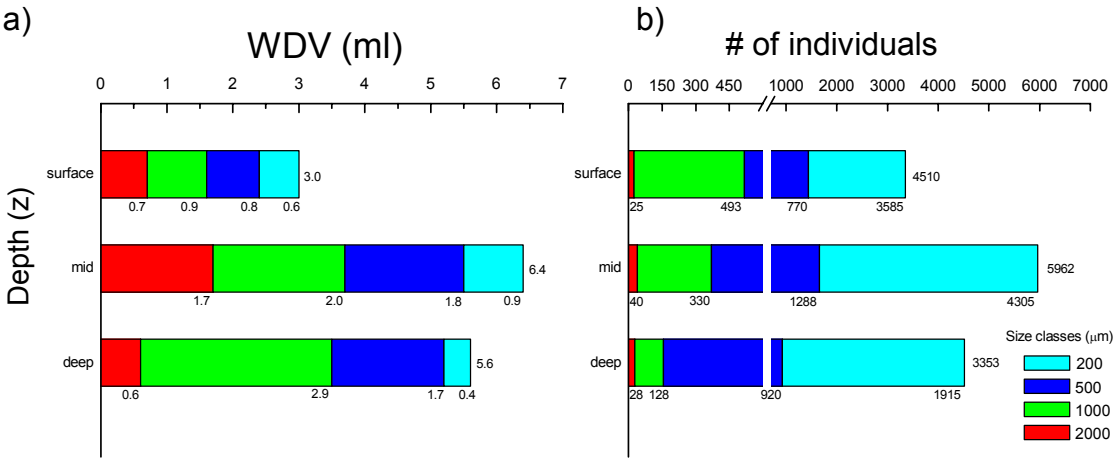

Figure 19. Biovolume (a) and all zooplankton group (b) vertical distribution during AS03 cruise.

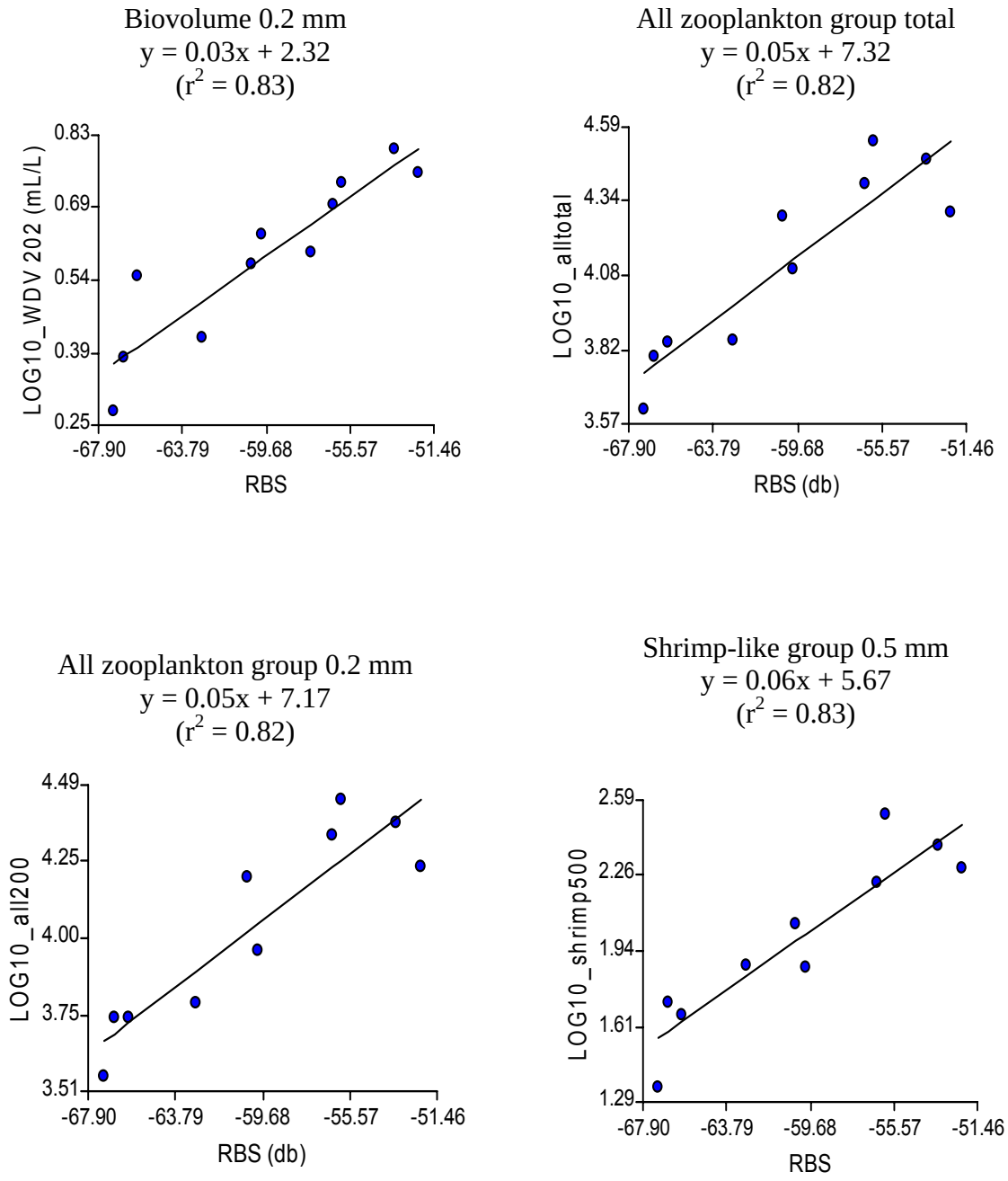

Figure 20. Regression models (I) (logx+1) during the MC cruise.

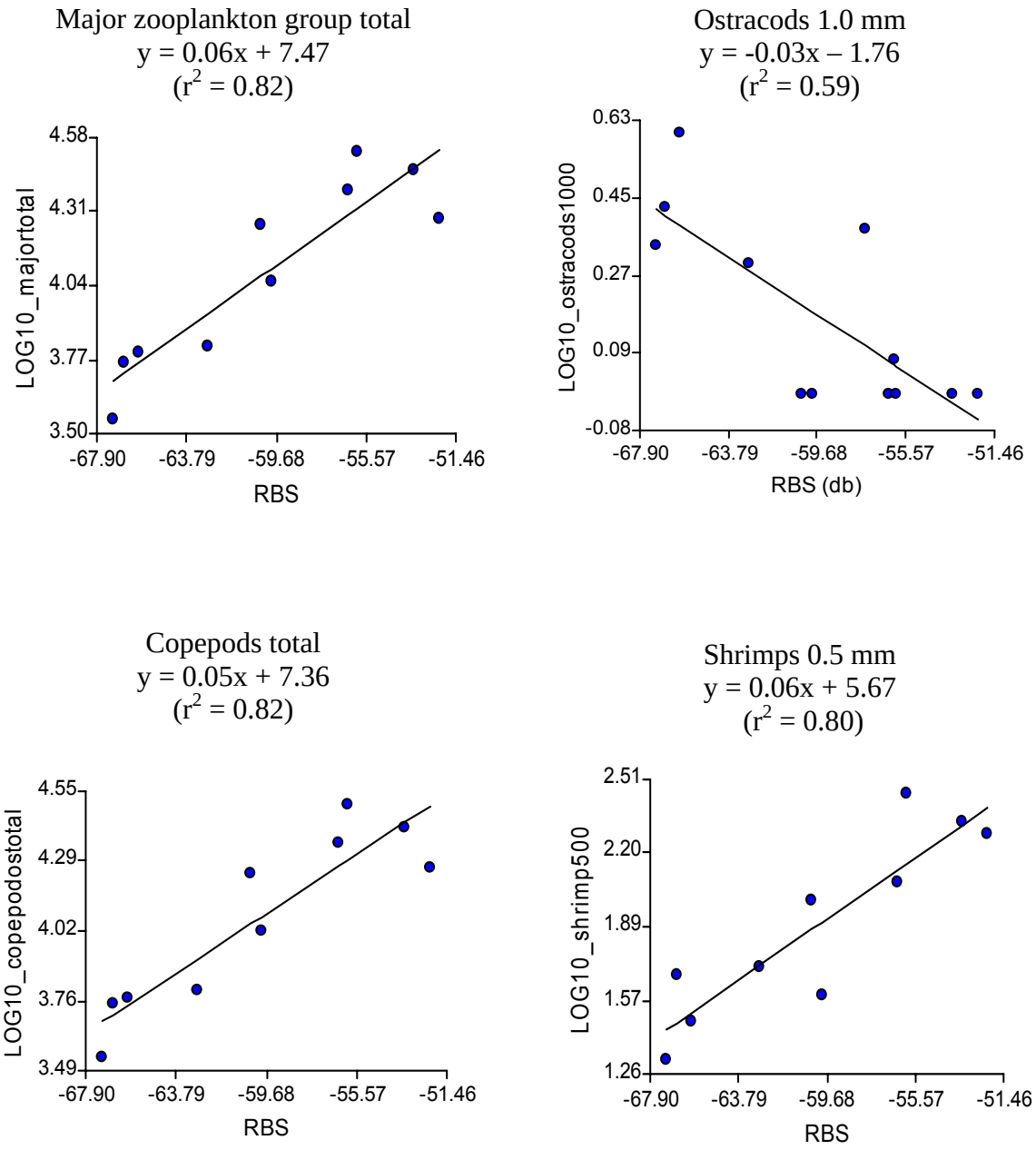

Figure 21. Regression models (II) (logx+1) during the MC cruise.

abundance between two depth layers. CTD profiles located the pycnocline at a depth of 70 to 90 m (Fig. 26). For most zooplankton groups smaller than 2.0 mm, the 0.5 mm net effectively fished more organisms than the 1.0 mm net (ANOVA; $p \leq 0.5$) (Table 6 and 11). No statistically significant differences between mesh sizes were found for marine organisms larger than 2 mm. The main component of the 1.0 mm net deep trawl was the shrimp-like group (amphipods, euphausiids, decapods, and unidentified shrimps) accounting for 60% of the whole collection. Among this group, the euphausiids *Stylocheiron abbreviatum*, *S. carinatum*, *S. longicorne*, *S. maximum*, *Euphausia americana*, *Nematoscelis atlantica*, *N. tenella*, and *E. tenera* were identified (Fig. 22).

Higher densities of most zooplankton groups and biovolumes were found at the upper 100 m layer, compared to the 100-200 m layer (ANOVA; $p \leq 0.05$) (Figs. 23-25 and Tables 6,11, and 12). The relative abundances of the main zooplankton components also varied between depth layers. At the deep layer, copepods and chaetognaths (major zooplankton group) represented 44%, siphonophores, ostracods, fish larvae, and gastropods (elastic group) 31%, and amphipods, euphausiids, and decapods (shrimp-like group) 25% of the total zooplankton/micronekton community. At the surface layer, copepods and chaetognaths accounted for 69%, amphipods, euphausiids, and decapods for 18%, and siphonophores, fish larvae, ostracods, and gastropods for 13% of the total zooplankton collection.

The Abril La Sierra 2004 bio-acoustic data gave the best available preliminary regressions for this study and the most robust regressions for the Abril La Sierra site. Several zooplankton/micronekton groups of size 1-2 mm (copepods $r^2 = 0.74$, chaetognaths $r^2 = 0.88$, gastropods $r^2 = 0.85$, and siphonophores $r^2 = 0.98$) and larger than 2 mm (copepods $r^2 = 0.83$, siphonophores $r^2 = 0.89$, and chaetognaths $r^2 = 0.82$) exhibited strong positive correlations with RBS (Table 13 and Figs. 28-31). In addition, the total abundance of the zooplankton/micronekton assemblage and biovolume of size 1-

2 mm showed statistically significant positive correlations with RBS (r^2 = 0.75 and 0.66, respectively). For biovolume and total zooplankton of size 1-2 mm the relationship implies that an increment of 1 dB corresponds to increments of approximately 0.3-1.5 ml of biovolume and 30-300 copepods per 60 m^3.

Table 11. Mean biovolumes and relative abundance (RA) during the AS04 cruise.

Variable (ml/100 m^3)	Mean		
	1.0 mm mesh 100-200 m (RA)	**0.5 mm mesh 100-200 m (RA)**	**0.5 mm mesh 0-100 m (RA)**
Biovolume 2.0 mm	0.77 (54.61)	1.14 (26.86)	2.74 (17.26)
Biovolume 1.0 mm	0.64 (45.39)	1.57 (36.88)	7.93 (49.93)
Biovolume 0.5 mm	-	1.54 (36.26)	5.21 (32.81)
Biovolume total	1.41 (-)	4.26 (-)	15.89 (-)

Table 12. One-way Analysis of Variance (ANOVA) procedures testing differences between (1) mesh size and (2) depth layers during the AS04 cruise. The "X" corresponds to statistically significant differences ($p \leq 0.05$).

Variable	1.0 vs. 0.5 mm (100-200 m)	0-100 m vs. 100-200 m (0.5 mm)
Biovolume 1.0 mm		X
Biovolume 0.5 mm		X
Biovolume total		X
All zooplankton group 2.0 mm		X
All zooplankton group 1.0 mm	X	X
All zooplankton group total	X	
Shrimp-like group total	X	
Elastic group 2.0 mm		X
Elastic group 1.0 mm		X
Elastic group total	X	
Major zooplankton group 2.0 mm		X
Major zooplankton group 1.0 mm	X	X
Major zooplankton group total	X	X
Amphipods 2.0 mm	X	
Brachyurans 2.0 mm		X
Brachyurans 1.0 mm		X

Table 12. Cont.

Variable	1.0 vs. 0.5 mm (100-200 m)	0-100 m vs. 100-200 m (0.5 mm)
Brachyurans total	X	
Carideans Total	X	
Cephalopods 1.0 mm		X
Cephalopods Total		X
Chaetognaths 2.0 mm		X
Chaetognaths 1.0 mm		X
Chaetognaths Total		X
Copepods 2.0 mm		X
Copepods 1.0 mm	X	X
Copepods Total	X	X
Gastropods 1.0 mm		X
Ostracods 1.0 mm	X	X
Ostracods 0.5 mm		X
Ostracods Total	X	X
Sergestids Total		X
Siphonophores 2.0 mm	X	X
Siphonophores 1.0 mm		X

Table 13. Zooplankton abundance and biovolumes regression models (logx+1) vs. relative backscatter strength (RBS) during the AS04 cruise.

Variable	Regression Model	R^2 Value	T-Value	P-Value
Biovolume 1.0 mm	0.08x + 5.26	0.66	4.40	0.0013
Biovolume total	0.09x + 5.96	0.56	3.58	0.0050
All zoo group 1.0 mm	0.15x + 11.26	0.75	4.59	0.0025
All zoo group total	0.14x + 10.84	0.48	2.57	0.0372
Elastic group 2.0 mm	0.13x + 8.55	0.88	7.31	0.0002
Elastic group 1.0 mm	0.14x + 9.50	0.94	10.67	<0.0001
Major zoo group 2.0 mm	0.14x + 9.51	0.83	5.76	0.0007
Major zoo group 1.0 mm	0.19x + 13.31	0.80	5.28	0.0012
Major zoo group total	0.18x + 12.87	0.52	2.74	0.0288
Amphipods 1.0 mm	0.07x + 5.03	0.49	2.57	0.0368
Chaetognaths 2.0 mm	0.13x + 8.92	0.82	5.70	0.0007
Chaetognaths 1.0 mm	0.17x + 11.33	0.88	7.25	0.0002
Chaetognaths total	0.16x + 11.16	0.59	3.20	0.0150
Copepods 2.0 mm	0.12x + 7.84	0.83	5.88	0.0006
Copepods 1.0 mm	0.20x + 13.96	0.74	4.42	0.0031
Copepods total	0.20x + 13.82	0.48	2.52	0.0398
Gastropods 1.0 mm	0.06x + 4.01	0.85	6.21	0.0004
Ostracods 0.5 mm	-0.18x – 9.33	0.74	-4.44	0.0030
Siphonophores 2.0 mm	0.14x + 8.85	0.89	7.62	< 0.0001

Table 13. Cont.

Variable	Regression Model	R^2 Value	T-Value	P-Value
Siphonophores 1.0 mm	0.15x + 10.23	0.98	16.92	< 0.0001
Siphonophores total	0.14x + 10.14	0.56	3.00	0.0199

Plate 10. *Stylocheiron longicorne*
(size > 1.0 cm)

Plate 11. *Stylocheiron maximum*
(size > 1.0 cm)

Plate 12. *Nematoscelis atlantica*
(size < 1.0 cm)

Plate 13. *Nematoscelis tenella*
(size < 1.0 cm)

Plate 14. *Euphausia americana*
(size < 1.0 cm)

Figure 22. Digital photographs (II) of several euphausiids collected during the zooplankton cruises.

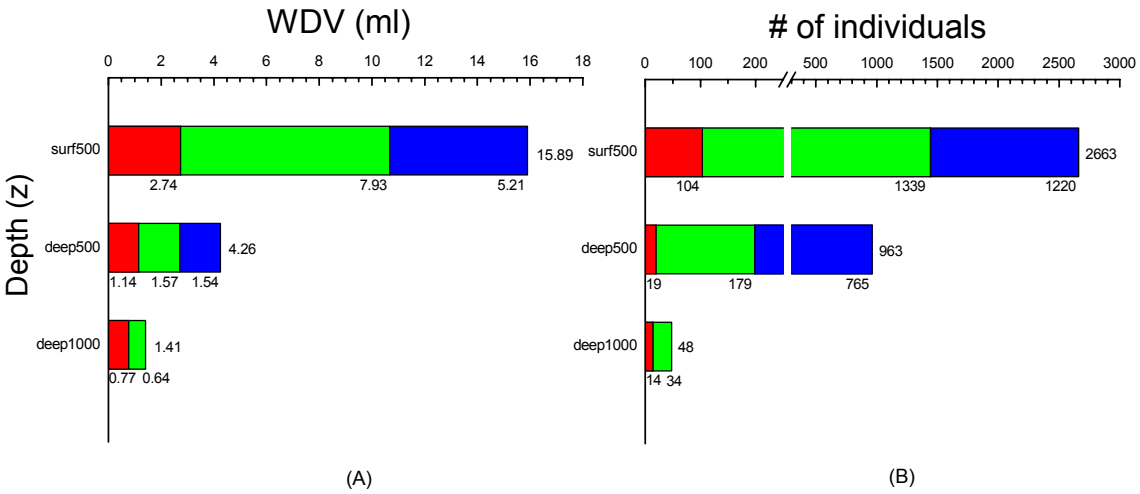

Figure 23. Vertical distribution of the biovolume (A) and total zooplankton (B) during AS04 cruise.

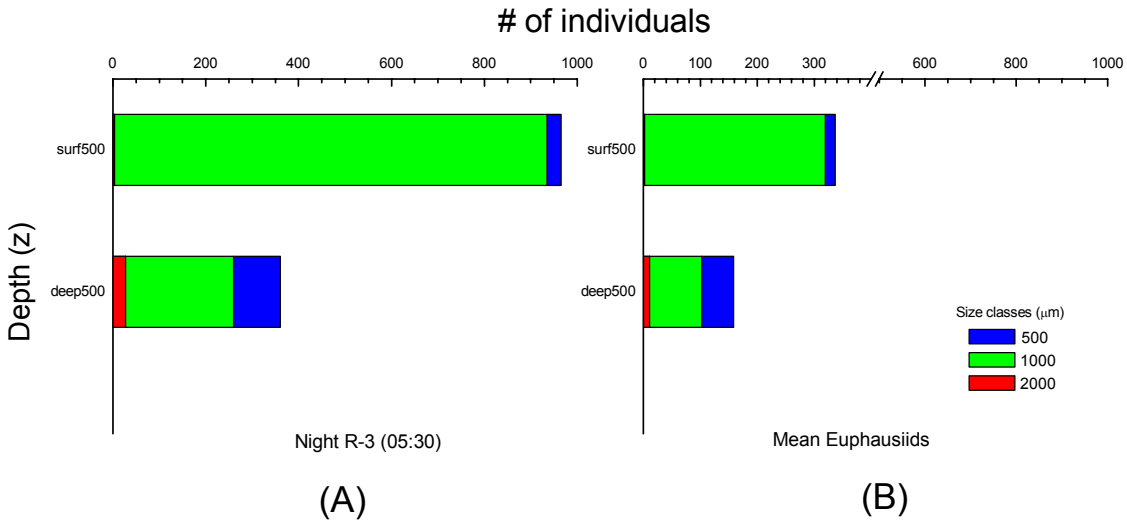

Figure 24. Abundance and vertical distribution of euphausiids showing large morning pulse during August replicate (A). Mean abundance and vertical distribution of euphausiids during the AS04 cruise (B).

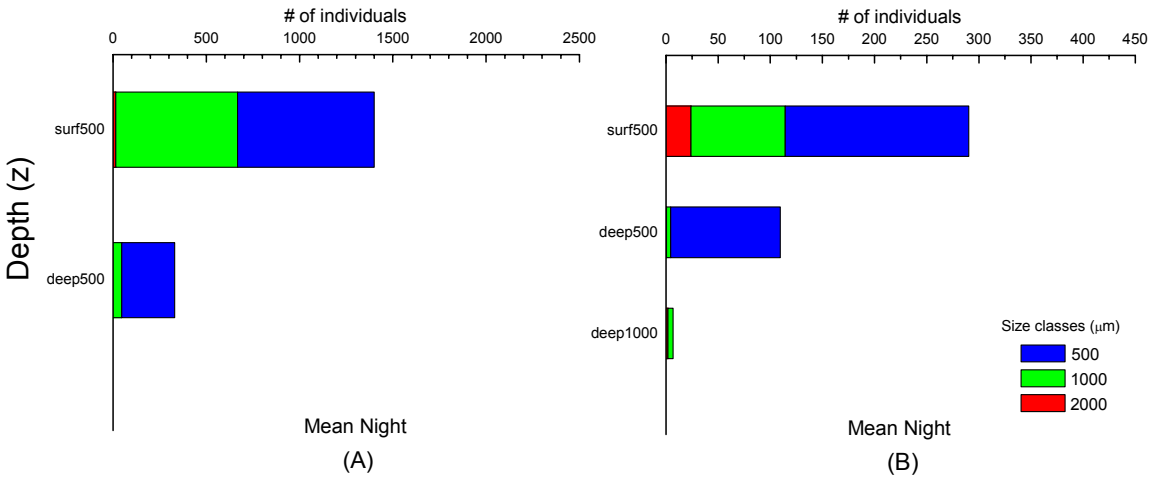

Figure 25. Abundance and vertical distribution of copepods (A) and siphonophores (B) during the AS04 cruise.

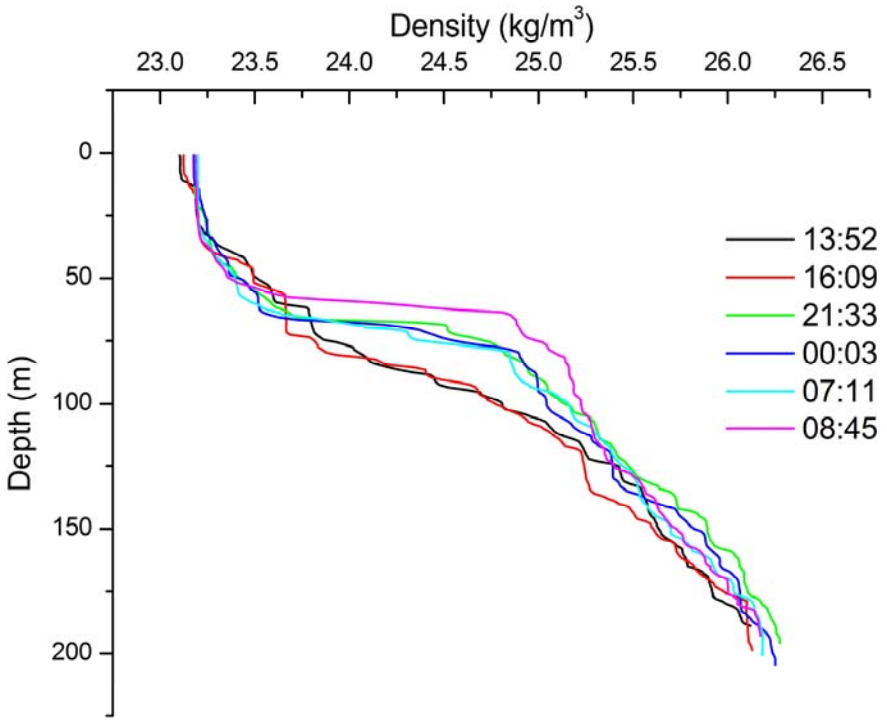

Figure 26. Density (σ_t) profiles during the AS04 cruise.

Figure 27. Net tow depth and temperature profiles during the AS04 cruise.

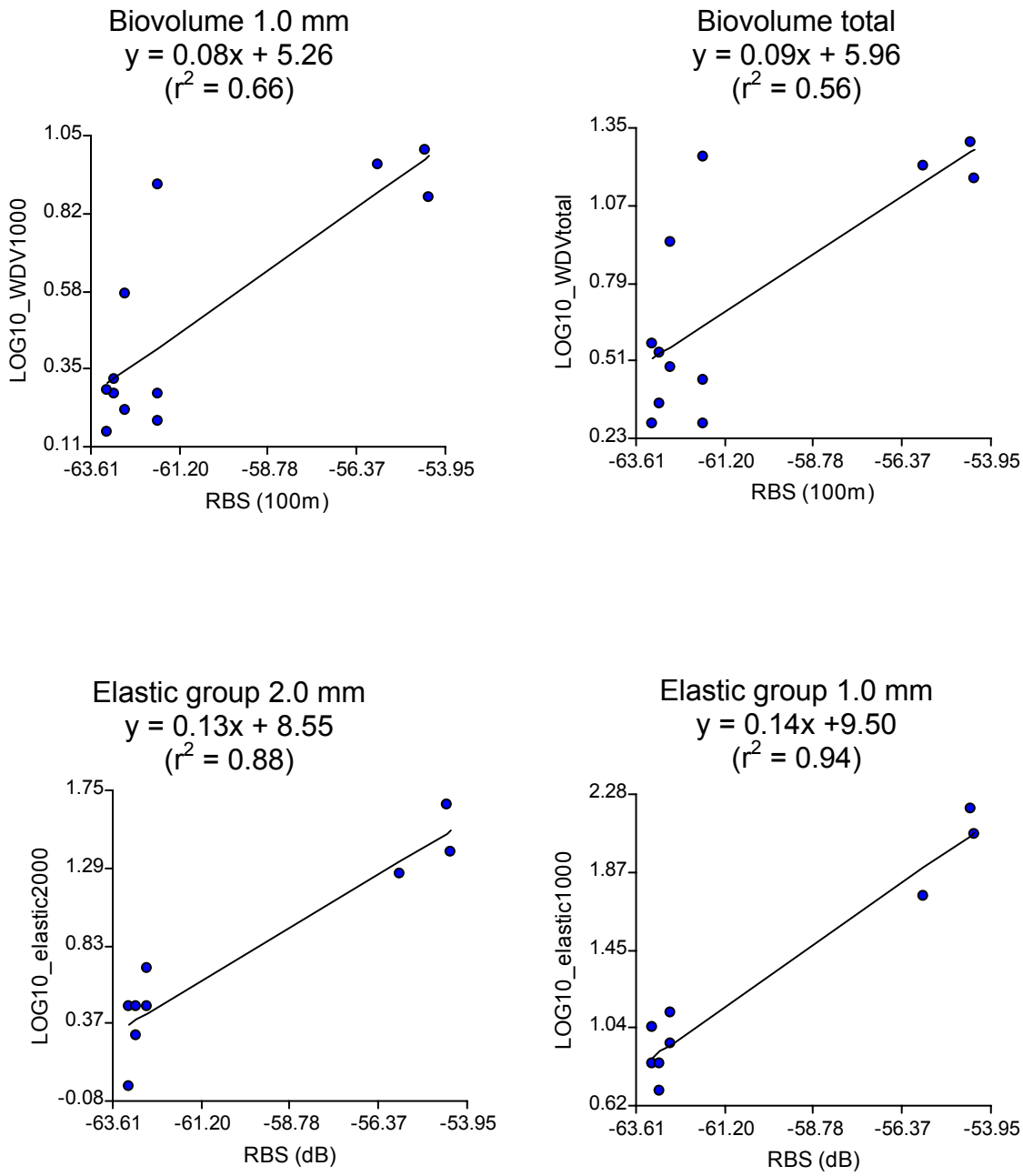

Figure 28. Regression models (I) (logx+1) during the AS04 cruise (biovolume size class 1.0 mm and total biovolume; elastic group, size classes 2.0 and 1.0 mm).

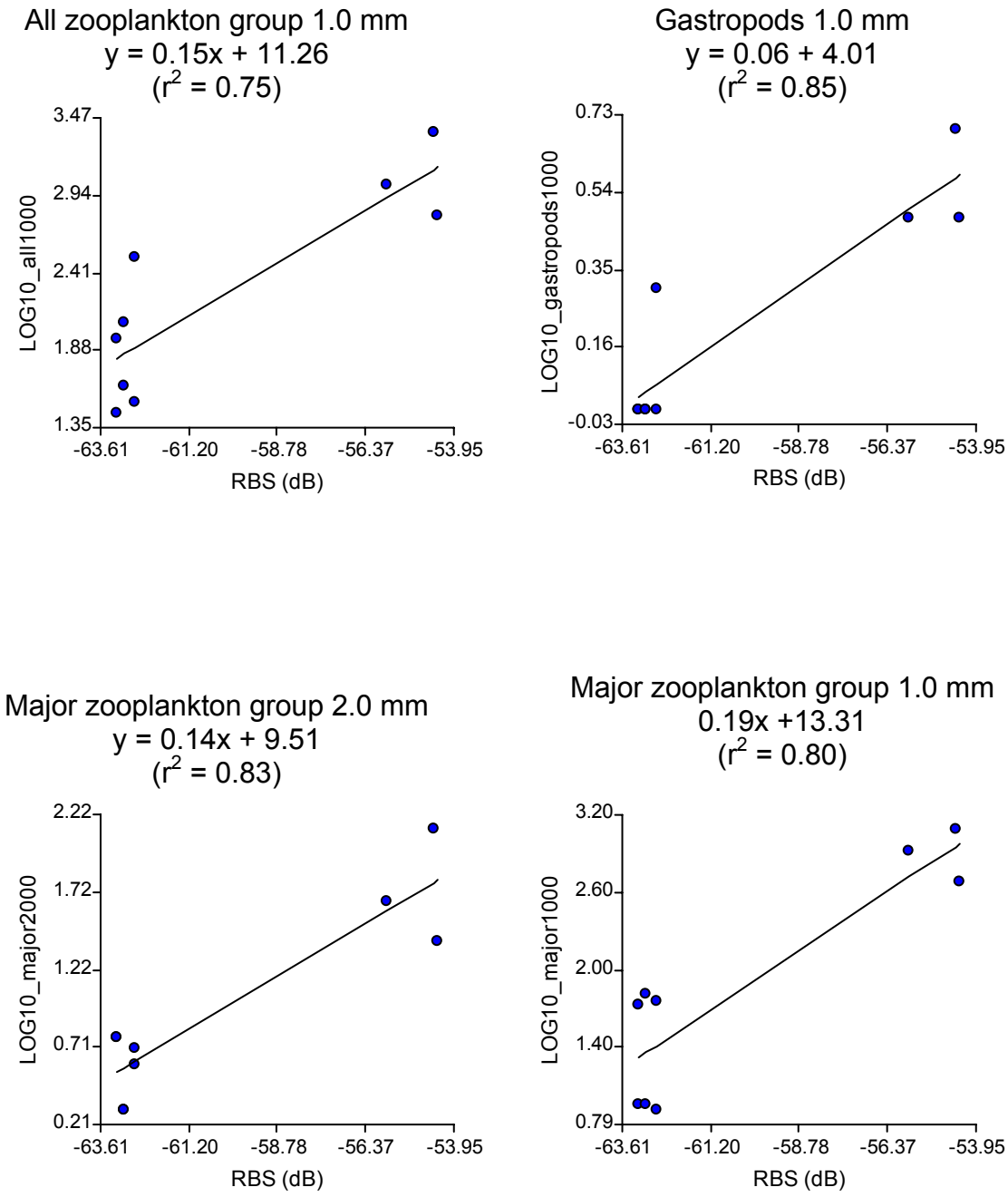

Figure 29. Regression models (II) (logx+1) during the AS04 cruise (all zooplankton group, gastropods, and major zooplankton group, size class 1.0 mm; and major zooplankton group size class 2.0 mm).

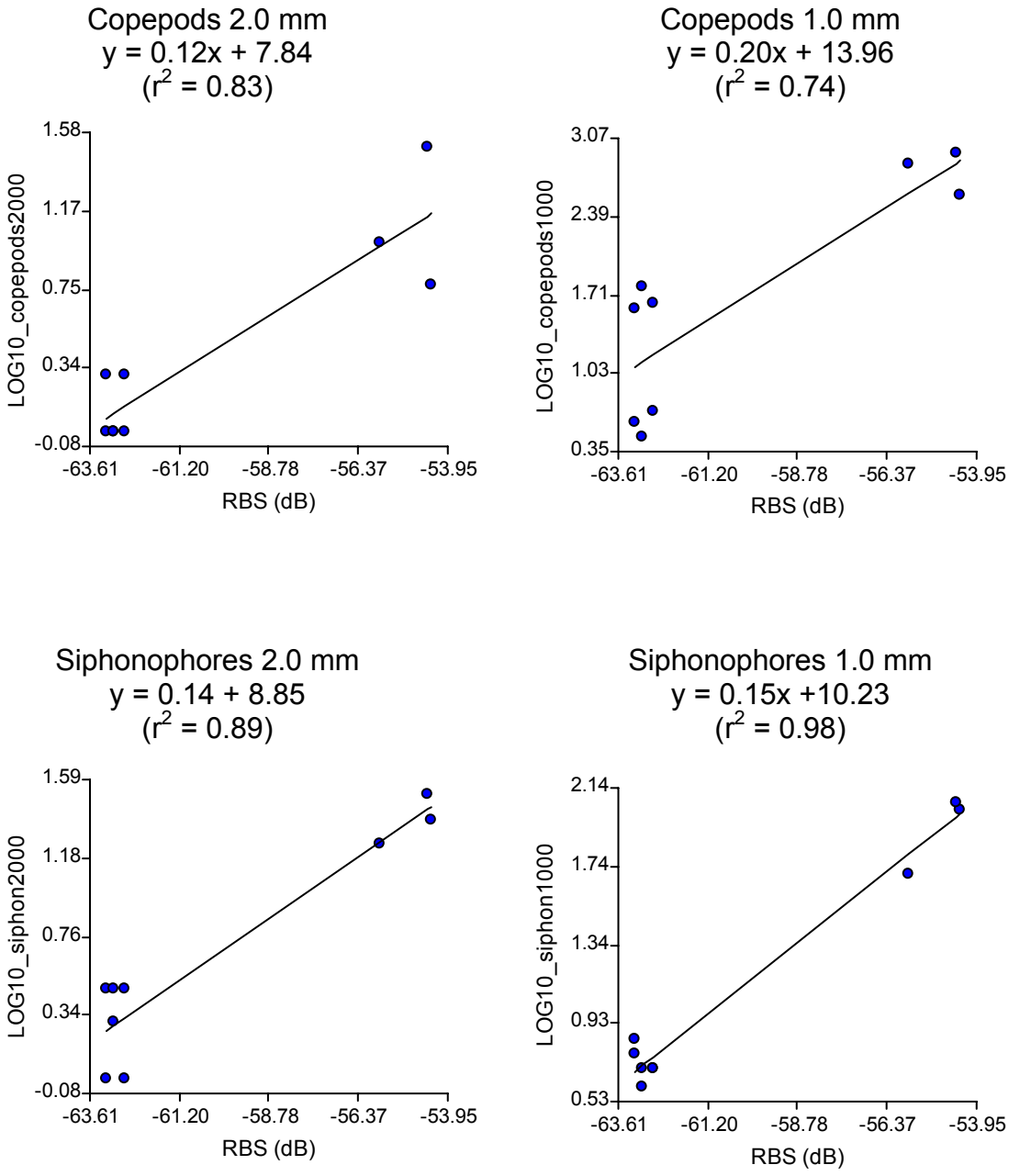

Figure 30. Regression models (III) (logx+1) during the AS04 cruise (copepods and siphonophores, size classes 2.0 and 1.0 mm).

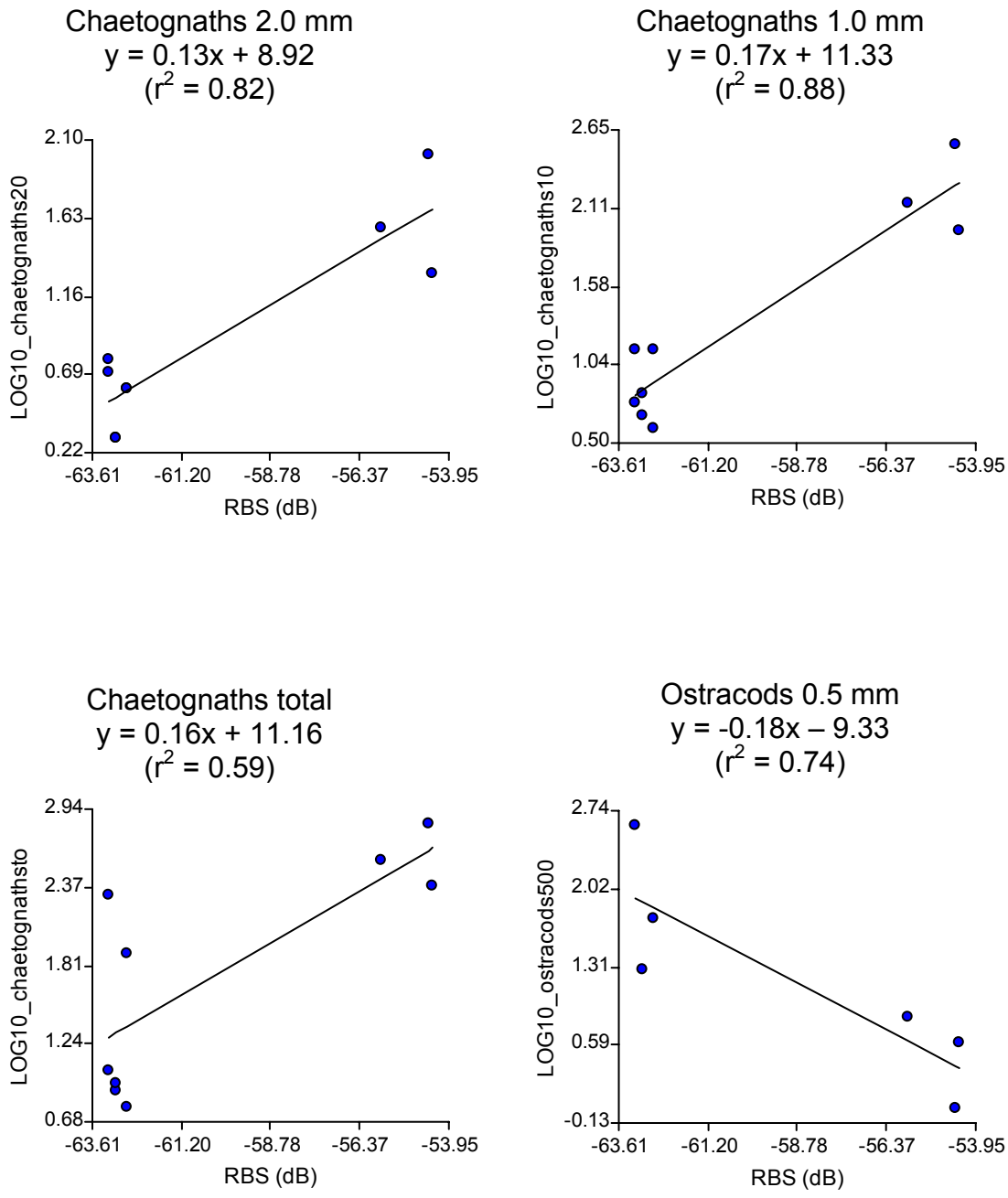

Figure 31. Regression models (IV) (logx+1) during the AS04 cruise (chaetognaths, size classes 2.0 mm and 1.0 mm, and total chaetognaths; ostracods size class 0.5 mm).

Discussion

Acoustic Data

The use of ADCP in marine research is relatively new and its primary purpose has been to obtain current velocity data. Because the primary objective of the MC, AS03 and AS04 deployments was to estimate larval fish pseudo-trajectories the ADCP was configured to obtain the best current data and ignored microstructures and patterns in the water column. Capella (personal communication) suggested that the best current velocity data were achieved during the AS04 deployment using a 10 meter bin, 60 pings per ensemble, and a 20 min sampling interval. Greenblatt (1981) suggested that an increase in the volume insonified (bin size) reduced bias in velocity estimates from large nektonic organisms. Also, an increased number of pings per ensemble represented better the real distribution of the current velocities.

On the other hand, for DVM pattern and structure recognition the best ADCP echo intensity data were obtained using parameters similar to those used in the PRG deployment. The reduced sampling interval in the PRG deployment allowed observation of microscale patterns in small time scales, such as DVM and RDVM behavior, which otherwise would be overlooked. Also, modifying (increasing or reducing) the bin size would have optimized resolution of specific organisms and/or layers. In all events, diel changes in relative backscatter strength were well documented.

Relative backscatter strength (RBS) time-series contours revealed the existence of microlayers at all sites. The best illustration of these layers was during the PRG deployment. The sharp spatio-temporal resolution during this event allowed clear recognition of microlayers associated with DVM and RDVM. The most conspicuous DVM layer followed a gradual ascent from depths of 400 m during dusk, but its dawn descent was steep and abrupt to similar depths.

This sharp vertical descent at dawn was also evidenced during MC and AS04. MC net tows (09:00 and 05:30) in the 120-180 m layer qualitatively corroborated that changes in RBS were associated with changes in total zooplankton abundance (Fig. 18). Maximum velocities associated with this layer were over 10 cm/s. Dr. Mark Ohman (personal discussion) suggested that the only migrators capable of achieving these speeds during vertical displacements are myctophids, cephalopods (small nekton), and to the least extent, large euphausiids. Alternatively, RDVM behavior has been explained as a counter mechanism of DVM predation. The RDVM layer was clearly exhibited during the PRG event at depths of 150 m. This diffuse layer gradually descended during the night, but at sunrise sprinted toward the surface layer at speeds of 4-6 cm/s, opposite to DVM. Light seems to be the principal cue for both DVM and RDVM behaviors.

Zooplankton Data

Of the three cruises analyzed during this study the MC cruise was the only one to yield enough data to describe significant differences of zooplankton abundance between day and night samples. Results based on net tows showed that organisms were more abundant during the day than night, in contrast to what would be expected from the RBS time-series contours. This could be an artifact of the mesh size used, limiting captures to the smallest spectrum of the zooplankton community. Larger organisms and probable scatterers, such as copepods, amphipods, and euphausiids, could have avoided nets more effectively. Therefore, these results could be interpreted as fewer organisms at night due to the fact of a stronger grazing pressure by predators capable of avoiding the nets. In addition, bottom-up mechanisms could be influencing zooplankton patchiness. Higher densities of organisms and biomass within the surface mixed layer suggest that the pycnocline may function as a barrier for

zooplankton distribution. Most subsurface biological interactions occur in the vicinity of the pycnocline.

The AS03 cruise was conducted during the early half day of March 18, 2003. If a general diel migration behavior was present, most of the organisms would have been found well below the surface layer. In fact, most 1-2 mm organisms and biovolumes were collected in the mid and deep strata. This size range comprises micronektic species like copepods and euphausiids which are known to be migrators. Most organisms in the smallest size range (0.5 to 0.3 mm) were most abundant at the mid stratum, while abundance decreased significantly at the deep stratum. Two mechanisms, a biological behavior and a physical barrier, could be playing important roles influencing daily patchiness. The fact that there were no night collections limited our understanding of diel zooplankton dynamics during this cruise.

Most samples during the AS04 cruise were collected at night. Mesh size comparisons showed that the smaller mesh size captured more organisms than the larger mesh. This would be expected given the fact that the majority of the zooplankton are within the smaller size range. On the other hand, larger organisms including migrants which comprise a small fraction of the whole community were probably not affected by mesh size. In fact, in order to target this size fraction of the zooplankton assemblage, the large mesh size (1 mm) seems to be more effective, capturing larger organisms and reducing bias from clogging of the net by small particles.

Due to the lack of day samples, it is difficult to establish if the pattern of higher zooplankton abundance in the surface layer was influenced by the physical barrier imposed by the pycnocline, or if there was any diel migrating behavior present. It should be noted that ostracods presented an opposite vertical distribution pattern of higher numbers at depths of 100-200 m during these night collections. One explanation could be the fact that they become passive and sink during the night due to no light stimulus and/or alternatively,

that they are performing RDVM, where they spend the day grazing at surface and at dusk descend to deeper waters to avoid diel migrating predators.

Regression Analysis of RBS and Zooplankton Abundance

The stronger regressions between RBS and zooplankton abundance were associated with the larger mesh size used. The best linear fit was achieved during the AS4 cruise. This is in agreement with a study by Greenblatt (1981) where a similar ADCP (87.6 kHz) having a size detection threshold of 2 mm was used. This value represents the upper limit of the net's capability during the AS04 cruise. During the MC cruise, the best regressions corresponded to biovolume and organisms within the size range of 0.2 to 0.5 mm. Although these organisms are extremely small for the ADCP sensitivity range, large compacted aggregations could in fact be resonant to the ADCP frequency. Otherwise, a top-down control mechanism could be operating where zooplankters, which increase RBS, could be preying on intermediate species, reducing grazing pressure, and therefore, influencing (increasing) microzooplankton biovolume and abundance.

During the AS03 cruise regressions showed a negative trend, where RBS increased as zooplankton biomass decreased. Since the sampling tow interval was relatively short, only two ADCP ensembles were used. Microscale zooplankton patchiness obtained from nets during short time intervals was underrepresented by the acoustic data acquisition settings. During the AS04 cruise, statistically significant positive linear regressions were obtained between RBS and the largest organisms collected. In theory, this would be expected since the smallest organisms detectable by the ADCP frequency in this study are roughly 1.0 mm or larger.

Even though the biological components of the scatter signal are not fully resolved, a valuable insight of the possible scatterers was achieved by the net vertical samplings of zooplankton and the vertical velocity profiles. A complex taxonomic assemblage of copepods, amphipods, euphausiids, decapods, ostracods, siphonophores and small fishes was sampled with traditional net tows. Most of these taxonomic groups have different vertical distributions and under certain conditions are known to migrate (Ohman, 1990). Their rate of migration should be influenced by their physiological constraints. For example, in the Parguera event the most likely taxonomic group capable of migrating from 400 to 50 m at a rate of 10 cm/s is small nekton, such as myctophids or small cephalopods. The evidently slower reverse migration could be associated to a complex assemblage of large copepods, euphausiids, decapods, amphipods, ostracods, and/or siphonophores.

Our taxonomic identification was focused on copepods and euphausiids, although a considerable number of organisms were decapods and amphipods. The large oceanic calanoid copepods *Candacia pachydactyla, Euchaeta marina, Undinula vulgaris,* and *Scolecithrix danae* are commonly encountered in tropical oceans. Brinton et al. (1999) described the taxonomy, ecology and distribution of the euphausiids discussed below in the interactive manual *Euphausiids of the World Ocean*, a compilation of most research efforts in this taxonomic group. All the identified euphausiids are considered important prey items of most zooplanktivorous fishes and whales encountered in tropical ocean basins (Brinton et al., 1999). The *Stylocheiron* spp presented a variety of sizes and vertical distributions. *Stylocheiron elongatum* (adult size 11.5–18.0 mm) lives at 200-500 m, deeper than any of the *S. longicorne* group. The smaller spp *S. longicorne* (adult size 7.0–11.3 mm) typically occurs below 140 m while the warm-water cosmopolitan spp *S. carinatum* (adult size 6.0–12.0 mm) inhabits the

upper 140 m during day and night (Brinton et al., 1999). The complex *S. affine* form (adult size 5.4-8.5 mm) occupying all tropical and subtropical seas beyond the continental/insular shelf appear to be a non-migrant, living in and above the thermocline.

A group of several *Euphausia* spps was positively identified. The most conspicuous among them were *E*. *tenera*, *E. brevis*, *E. americana*, and *E. mutica*. With the exception of *E. americana*, all other *Euphausia* spps are considered vertical migrators. *Euphausia tenera* (adult size 7.0-9.0 mm) adults spend their daytime at depths of 150 -300 m and at night above 140 m in a layer at 50-75 m (Brinton et al., 1999). *Euphausia mutica* (adult size 7.0-12.0) have a deeper day distribution at depths of 300-400 m and ascend above 50 m at night. *Euphausia brevis* (adult size 8.0-10.0 mm) occurs above 100 m at night but descend below 300 m during daylight (Brinton et al., 1999). Two species of *Nematoscelis* were identified: *Nematoscelis atlantica* and *N. tenella*. *Nematoscelis atlantica* occurs at the Atlantic Ocean between the 40° parallels, widespread at the Mediterranean Sea, but rarely recorded from the tropical Atlantic. *Nematoscelis atlantica* (adult size 10.0-15.0 mm) adults are mostly distributed below 250 m during the day and above it at night. *Nematoscelis tenella* (adult size 13.0-20.0) a tropical-subtropical oceanic species lives deeper, where juveniles and adults occur throughout about 100-450 m during the night and at 200-450 m by day. Most immature and larvae of *N. atlantica* are above 50 m day and night, *N. tenella* larvae lives above the thermocline at about 100 m (Brinton et al., 1999).

An abundant and large species collected was *Stylocheiron abbreviatum* (adult size 12.0–17.0 mm) occurring at a depth of 50-300 m day and night. Another large species collected was *S. maximum* (adult size 20.0-30.0 mm), a widespread mesopelagic species rarely found above 150 m. A relatively large tropical *Thysonopoda* spp found was *Thysonopoda tricuspidata* (adult size 15.0–25.0 mm) but only furcilia and juvenile stages were collected. Considered

oceanic and a strong vertical migrator, they occur above the thermocline at night and below 300 m by day, probably associated with deep scattering layers and DVM. A peculiarly large euphausiid catch was obtained during the night tow of August 9, 2004 with a total of 359 individuals at the mid layer tow and 966 individuals at the surface layer (Fig. 24). The increased number could be attributed to several factors: the net tow was collected during the morning twilight hours when organisms started their descent to deep waters, the use of a wider mesh size allowed a faster trawl in the opposite direction of the downward migration, and/or a pulse or patch was encountered during the net tow.

Conclusions and Recommendations

1. The simultaneous approach of an acoustic method (RBS-ADCP) and discrete zooplankton/micronekton samples supports the presence of a biologically produced “deep scattering layer” in the Mona Passage and La Parguera shelf/slope habitats.
2. The vertical displacement of RBS time-series contours are consistent with zooplankton/micronekton diel migratory behavior, but discrete samples only detected higher abundance at the deepest layer on night samplings (avoidance effects).
3. The diel vertical migration appears to be light regulated, with maximum vertical displacements associated with sunrise and sunset.
4. Reverse diel vertical migrators (RDVM) observed during PRG cruise may be associated with the presence of zooplanktivorous predators, which could have influenced the RBS in all events but were not collected in net samples due to their increased avoidance abilities.
5. Zooplankton abundance and vertical distribution was associated with the pycnocline. Most microlayers bio-dynamics occur around this density gradient.
6. The MC and AS04 bio-acoustic data provided robust preliminary regressions between RBS and zooplankton abundance for this study.
7. Future surveys should consider the use of optical plankton counters (OPC) or video plankton recorders (VPR) as a means to improve spatial and temporal resolution, provide stronger relationship between RBS and biological components, and to increase our understanding of microlayers dynamics.

8. Traditional net tows are still the best approach to identify organisms to a species level and are useful when calibrating acoustic and optical sensing systems.
9. ADCP's RBS time-series demonstrate the effectiveness of acoustics as indirect approaches for marine bio-dynamics research. They can be used as a standard tool for preliminary assessments, reducing research time and costs; and/or as a complimentary instrument improving space and time resolution for plankton/nekton research.

Literature cited

Attenborough, D. 2002. The Blue Planet – Seas of Life Collector Set [DVD Documentary]. London: BBC Video.

Baird, R.W., A.D. Ligon, S.K. Hooker, and A.M. Gorgone. 2001. Subsurface and nighttime behaviour of pantropical spotted dolphins in Hawaii. Can. J. Zool. 79: 988-996.

Batchelder, H.P., J.R. Vankeuren, R. Vaillancourt, E. Swift. 1995. Spatial and temporal distributions of acoustically estimated zooplankton biomass near the Marine Light-Mixed Layers station (59º 30' N, 21º 00' W) in the North Atlantic in May 1991. Journal of Geophysical Research. 100 (C4): 6549-6562.

Brinton, E., M. D. Ohman, A.W. Townsend, M.D. Knight, and A.L. Bridgeman. 1999. Euphausiids of the World Ocean [CD-ROM]. Amsterdam: ETI.

Calef G.W. and G.D. Grice. 1967. Influence of the Amazon River Outflow on the Ecology of the Western Tropical Atlantic II Zooplankton Abundance, Copepod Distribution, with Remarks on the Fauna of Low-salinity Areas. Journal of Marine Research. 25: 84-94.

Corredor, J.E., J.M. Morell, J.M. López, J.E. Capella, and R.A. Armstrong. 2004. Cyclonic Eddy Entrains Orinoco River in Eastern Caribbean. EOS 85 (20): 197-208.

Deines, K.L. 1999. Backscatter estimation using broadband acoustic Doppler profilers. In: Anderson, S.P., et al. (Eds.). Proceedings of the IEEE Sixth Working Conference on Current Measurement, March 11-13, 1999. San Diego, CA. 249-253 pp.

De Robertis, A. 2002. Size-dependent visual predation risk and the timing of vertical migration: An optimization model. Limnology and Oceanography. 47 (4): 925-933.

Esteves, R.F. 2005. Dispersal of Reef Fish Larvae from Known Spawning Sites in La Parguera. Unpublished masters Dissertion. University of Puerto Rico. Mayaguez, PR. 53 pp.

Flagg, C.N. and S.L. Smith. 1989. On the use of the acoustic Doppler current profiler to measure zooplankton abundance. Deep Sea Research. 36 (3): 455-474.

García-Sais, J.R., R. Appeldoorn, A. Bruckner, C. Caldow, J.D. Christensen, C. Lilyestrom, M.E. Monaco, J. Sabater, E. Williams, and E. Díaz. 2005. The State of Coral Reef Ecosystems of the Commonwealth of Puerto Rico. In: J. Waddell (ed.), The State of Coral Reefs Ecosystems of the United States and Pacific Freely Associated States: NOAA technical Memorandum NOS NCCOS II. NOAA/NCCOS Center for Coastal Monitoring and Assessment's Biogeography Team. Silver Spring, MD. 91-134 pp.

García-Sais, J., J.E., Capella, J. Rojas, and R. Esteves. 2003. Dispersal of Reef Fish Larvae from Known Spawning Sites in Mayaguez and La Parguera. Department of Marine Sciences-UPRM. NMFS Final Report. 97 pp.

González-Figueroa, A.J. 2002. Vertical and temporal distribution patterns and taxonomic composition of ichthyoplankton and zooplankton off the insular shelf-edge of Guayanilla Bay, southwest Puerto Rico. Unpublished Masters Dissertation. University of Puerto Rico. Mayaguez, PR. 88 pp.

Greenblatt, P. 1981. Sources of acoustic backscattering at 87.5 kHz. J. Acoust. Soc. Am. 70 (1): 134-142.

Greene C.H., P.H. Wiebe, and J.E. Zamon. 1994. Acoustic Visualization of Patch Dynamics in Oceanic Ecosystems. Oceanography. 7 (1): 4-12.

Grubbs, R.D., K.N. Holland, and D.G. Itano. 2001. Foods habits and trophic dynamics of structure-associated aggregations of yellowfin and bigeye tuna (*Thunnus albacares* and *Thunnus obesus*) in the Hawaiian Islands: Project description, rationale and preliminary results. Yellowfin Research Group-SCTB 14. Noumea, New Caledonia.

Johnson, H.R., R.H. Backus, J.B. Hersey, and D.M. Owen. 1956. Suspended echo-sounder and camera studies of midwater sound scatterers. Deep Sea Research. 3: 266-272.

Michel, H.B., M. Foyo, and D.A. Haagensen. 1976. Caribbean Zooplankton. Superintendent of Documents-U.S. Government Printing Office, Washington D.C., USA, 712 pp.

Nelson, W.R. and R.S. Appeldoorn. 1985. Cruise Report R/V Seward Johnson. A submersible survey of the continental slope of Puerto Rico and the US Virgin Islands. Report submitted to NOAA, NMFS, SEFC, Mississippi Laboratories. University of Puerto Rico, Department of Marine Sciences. 76 pp.

Ohman, M.D. 1990. The demographic benefits of diel vertical migration by zooplankton. Ecol. Monogr. 60 (3): 257-281.

Pabón-Valentín, A.E. 2001. Variations of Zooplankton Community Structure across a neritic-oceanic gradient off La Parguera, Puerto Rico. University of Puerto Rico. Mayaguez, PR. 56 pp.

Ramirez-Mella, J.T. 2000. Cross-shelf distribution patterns of ichthyoplankton in La Parguera Bay and adjacent oceanic waters, southwest coast of PR. Unpublished Masters Dissertation. University of Puerto Rico. Mayaguez, PR. 111 pp.

Ramírez-Mella, J.T. and J.R. García-Sais. 2003. Offshore Dispersal of Caribbean Reef Fish Larvae: How Far Is It? Bulletin of Marine Science. 72 (3): 997-1017.

Richards, S.A., H.P. Possingham, and J. Noye. 1996. Diel vertical migration: modeling light-mediated mechanisms. Journal of Plankton Research. 18 (12): 2199-2222.

R.D. Instruments, 1996. Acoustic Doppler current profilers. Principles of Operation: a practical primer. R.D. Instruments. San Diego, CA. 54 pp. http://www.rdinstruments.com

Rojas-Ortega, J. 2002. Caracterización del ictioplancton a través del Canal de la Mona, con énfasis en familiares arrecifales. Unpublished Masters Dissertation. University of Puerto Rico. Mayaguez, PR. 69 pp.

Sameoto, D.D. 1983. Micronekton Sampling using a New Multiple-Net Sampler, the BIONESS, in Conjunction with a 120 kHz Sounder. Biological Oceanography. 2 (2, 3, and 4): 179-198.

Schnetzer, A. and D.K. Steinberg. 2002. Active transport of particulate organic carbon and nitrogen by vertically migrating zooplankton in the Sargasso Sea. Marine Ecology Progress Series. 234: 71-84.

Segura, W. 2000. Low frequency transport components in Mona Passage. Unpublished Doctoral Dissertation. University of Puerto Rico. Mayaguez, PR. 330 pp.

Sindlinger, L.R., D.C. Biggs, and S.F. Dimarco. 2005. Temporal and spatial variability of ADCP backscatter on a continental slope. Continental Shelf Research. 25: 259-275.

Stanton, T.K., D. Chu, and P.H. Wiebe.1996. Acoustic scattering characteristics of several zooplankton groups. ICES Journal of Marine Science. 53: 289-295.

Stanton, T.K., D. Chu. 2000. Review and recommendations for the modeling of acoustic scattering by fluid-like elongated zooplankton: euphausiids and copepods. ICES Journal of Marine Science, 57: 793-807.

Yoshioka, P.M., G.P. Owen, and D. Pesante. 1985. Spatial and Temporal Variations of oceanic Zooplankton near Puerto Rico. Final Report submitted to DOE/OHER/Center for Energy and Environmental Research, UPR-Marine Ecology Division. Mayaguez, PR.